RESERVOIR CHARACTERIZATION AND WATERFLOOD PERFORMANCE EVALUATION OF GRANITE WASH FORMATION, ANADARKO BASIN

A Thesis

by

AKSHAY ANAND NILANGEKAR

Submitted to the Office of Graduate and Professional Studies of
Texas A&M University
in partial fulfillment of the requirements for the degree of

MASTER OF SCIENCE

Chair of Committee,	David S. Schechter
Co-Chair of Committee,	Christine Ehlig-Economides
Committee Member,	Yuefeng Sun
Head of Department,	A. Daniel Hill

May 2014

Major Subject: Petroleum Engineering

Copyright 2014 Akshay Anand Nilangekar

ABSTRACT

The Granite wash formation in the Anadarko basin is classified as a tight-gas play and is located along the Texas – Oklahoma border. It has a complex mineralogy and consists of stacked-pay series of tight sands. Our zone of interest is the liquid-rich Missourian Wash B interval in Wheeler County in which two horizontal wells have been drilled. The purpose of this research is to characterize the reservoir through geologic modeling and determine the feasibility of a waterflood using simulation studies.

A set of field data was provided by the operator and other necessary parameters were obtained through publicly available field studies and literature. The final objective is implementing advanced reservoir simulation to integrate well log data, PVT data, diagnostic fracture injection test and microseismic analysis into a plan of development.

The Missourian Wash B formation has a maximum net pay thickness of 50ft. The target sand is laterally continuous which makes it an ideal horizontal drilling prospect. The wells are stimulated by multi-stage hydraulic fracturing. The initial production gas-oil ratio is 1800 scf/stb and PVT reports indicate presence of an oil reservoir above bubble point pressure. PVT correlations show that the 42º API oil and potential injection water at the reservoir temperature have almost the same viscosity. All these factors point towards the formation being a good waterflood candidate.

Well log analysis was performed to obtain porosity and saturation estimates. The microseismic mapping report provides a good overview of the well completion

efficiency. Laboratory PVT data was tuned to predict reservoir fluid behavior by parameter regression and component lumping. An isotropic black-oil simulator by Computer Modeling Group Ltd was selected for our work. The reservoir model was validated by sensitivity studies and history matching of production rates was performed.

Simulation result of waterflood implementation by utilizing offset horizontal wells as injectors is analyzed, and three different plans of development are discussed. It is seen that the overall response to waterflooding is poor due to low formation permeability leading to low water injectivity. But a greater reservoir area can be drained if production is initiated from additional horizontal wells. A well-spacing of four horizontal wells in 600 acres section is recommended. The stimulated reservoir volumes of adjacent wells should be close to each other for effective reservoir drainage.

DEDICATION

I dedicate this work to my dear parents, Anand and Shubhangi Nilangekar, for their undying encouragement and love.

ACKNOWLEDGEMENTS

I would like to thank my committee chair, Dr. David Schechter, my co-chair Dr. Christine Ehlig-Economides, and Dr. Yuefeng Sun for their guidance and support throughout the course of this research.

Thanks to all my research colleagues and department faculty and staff for making my time at Texas A&M University a great experience. A special mention for my Nagle Street group of friends for all the great time spent in their company and making my stay in College Station truly memorable. I also want to extend my gratitude to the Computer Modeling Group (CMG) and K.Patel for the training and assistance they provided me.

Finally, thanks to my family and friends back home for their patience and support.

TABLE OF CONTENTS

Page

ABSTRACT ii

DEDICATION iv

ACKNOWLEDGEMENTS v

TABLE OF CONTENTS vi

LIST OF FIGURES viii

LIST OF TABLES xii

CHAPTER I INTRODUCTION 1

1.1 Project Overview 2
1.2 Research Objectives 3
1.3 Thesis Outline 3

CHAPTER II LITERATURE REVIEW 5

2.1 Tight Oil 6
2.2 Horizontal Well Technology 9
2.3 Hydraulic Fracturing 10
2.4 Horizontal Well with Multi-stage Hydraulic Fracturing 12
2.5 Flow Patterns in Hydraulically Fractured Wells 13
2.6 Water Injection 14
2.7 Microseismic Monitoring 16

CHAPTER III GRANITE WASH PLAY 18

3.1 Geologic Setting 18
3.2 Mineralogy 20
3.3 Hydrocarbon Zones in the Granite Wash 22
3.4 Missourian Series Wash 23
3.5 Granite Wash Completions 25

Page

CHAPTER IV PETROPHYSICAL ANALYSIS 28

4.1 Methodology 31

CHAPTER V DIAGNOSTIC FRACTURE INJECTION TEST ANALYSIS 34

5.1 Methodology 34
5.2 DFIT Report Analysis and Results 36

CHAPTER VI MICROSEISMIC MONITORING REPORT ANALYSIS 40

6.1 Microseismic Fracture Map Analysis and Discussion 40

CHAPTER VII RESERVOIR MODEL DEVELOPMENT AND SIMULATION 46

7.1 Introduction 46
7.2 Reservoir Model 48
7.3 Symmetry Model Validation 53
7.4 Sensitivity Studies 54
7.4.1 Fracture Half-Length 55
7.4.2 Matrix Permeability 57
7.4.3 Rock Compressibility 59
7.5 History Match 61

CHAPTER VIII WATERFLOODING TEST AND DEVELOPMENT PLANS 70

8.1 Description of Waterflooding Model 70
8.2 Water Flooding Plans 71
8.2.1 Water Flood Plan 1 71
8.2.2 Water Flood Plan 2 76
8.2.3 Water Flood Plan 3 78
8.3 Summary 82

CHAPTER IX CONCLUSIONS AND RECOMMENDATIONS 84

9.1 Conclusions 84
9.2 Recommendations for Future Work 86

REFERENCES 87

LIST OF FIGURES

Page

Figure 1: Worldwide hydrocarbon resource distribution (CGG) 2

Figure 2: Unconventional resources triangle (Holditch. 2006) 5

Figure 3: Conventional sandstone cross-section (Naik. 2003) 7

Figure 4: Tight sand cross-section (Naik. 2003) 8

Figure 5: Tight oil plays in USA (IHS) 9

Figure 6: Hydraulic fracturing process 12

Figure 7: Multi-stage hydraulic fracturing (FracStim) 13

Figure 8: Types of flow in fractured horizontal well 14

Figure 9: Standard waterflood schematic (Shah et al. 2010) 15

Figure 10: Microseismic monitoring schematic (Maxwell, 2011) 16

Figure 11: Anadarko basin stratigraphic cross-section (Srinivasan et al. 2011) 19

Figure 12: Granite Wash deposition model 20

Figure 13: Mineral content of Granite Wash (OGS, 2003) 21

Figure 14: Grain Density of Granite Wash (OGS, 2003) 22

Figure 15: Granite Wash reservoirs and hydrocarbon type (Linn Energy) 23

Figure 16: Stratigraphic zonation of Granite Wash highlighting the Missourian Wash series (Mitchell, 2011) 25

Figure 17: Permitted horizontal wells till first quarter of 2011 (Mitchell, 2011) 26

Figure 18: Flowchart showing petrophyscial analysis sequence 28

Page

Figure 19: Missourian Wash "B" cross-section stratigraphy across vertical wells in the field (Operator data) 29

Figure 20: The well-log template of a zone in Well-1 lateral section 30

Figure 21: The induced fracture bypasses near well-bore damage and connects to the reservoir interval (Fekete, 2011) 35

Figure 22: Typical DFIT pressure response (Fekete, 2011) 36

Figure 23: Casing pressure and slurry rate and eventual fall-off plotted against time (DFIT report) 37

Figure 24: After closure analysis - Cartesian pseudoradial plot (DFIT report, 2011) 39

Figure 25: Well-1 microseismic activity top view (Microseismic mapping report) 41

Figure 26: Microseismic scatter side view (Microseismic mapping report) 42

Figure 27: Microseismic report review depicting the complex nature of events detected. An attempt is made to map planar fracture geometry across some stages 43

Figure 28: Stage 3 top view of microseismic mapping result, with the extent of major microseismicity 44

Figure 29: Stage 3 side view of microseismic activity 45

Figure 30: Transverse fractures in a horizontal well (Bo Song et al. 2011) 47

Figure 31: Base reservoir 3-D model 49

Figure 32: Reservoir Model Top view 50

Figure 33: One stage each of Well-1 and Well-2 51

Figure 34: Half-lengths of hydraulic fractures 52

Figure 35: Validation of symmetry model with comparison to actual base model. Average Reservoir pressure and cumulative rate are plotted. 54

Page

Figure 36: Sensitivity to fracture half-length: average reservoir pressure response to fracture half-length change....56

Figure 37: Sensitivity to fracture half-length: cumulative production trends with change in fracture half-length....56

Figure 38: Sensitivity to matrix permeability: average reservoir pressure response 57

Figure 39: Sensitivity to matrix permeability: cumulative production trends with change in matrix permeability....58

Figure 40: Sensitivity to rock compressibility: average reservoir pressure trends 59

Figure 41: Sensitivity to rock compressibility: cumulative production trends 60

Figure 42: Well-1 historical oil rate 63

Figure 43: Well-1 field and simulated Gas-Oil Ratio (GOR) 64

Figure 44: Actual and simulated water-rate profiles of Well-1 65

Figure 45: Simulated bottomhole pressure profile of Well-1 66

Figure 46: Historical oil-rate of Well-1....67

Figure 47: Actual field GOR and simulated GOR comparison 68

Figure 48: Water-rate history match for Well-2....68

Figure 49: Simulated bottomhole pressure profile of Well-2 69

Figure 50: Waterflooding symmetry model description, with two horizontal wells drilled on the exterior side of Well-1 and Well-2 71

Figure 51: Waterflood plan 1 average reservoir pressure profile....72

Figure 52: Cumulative oil production of waterflood plan 1....73

Figure 53: Average reservoir pressure profile as a function of time....74

Figure 54: Oil saturation after primary depletion and post-waterflood implementation..75

Page

Figure 55: Water saturation profile as a function of time 75

Figure 56: Average reservoir pressure profile for waterflood plan-2 77

Figure 57: Cumulative production from waterflood plan 2 compared with primary recovery 77

Figure 58: Water saturation profile as a function of time 78

Figure 59: Oil saturation profile as a function of time 78

Figure 60: Average reservoir pressure profile for waterflood plan 3 79

Figure 61: Cumulative oil production from waterflood plan 3 80

Figure 62: Reservoir pressure profile changes as a function of time 81

Figure 63: Oil saturation profile map before and after water injection 82

Figure 64: Water saturation profiles before and after injection 82

LIST OF TABLES

Page

Table 1: Petrophysical Analysis Summary 33

Table 2: Reservoir Properties of the Granite Wash Formation Field 61

Table 3: Fracture Properties of Well-1 and Well-2 61

Table 4: PVT Properties of the Reservoir Fluid Used in the Simulation Model 62

Table 5: Waterflooding Plans Summary 83

CHAPTER I

INTRODUCTION

Unconventional resources have attained a significant role in oil and gas production due to dearth of conventional hydrocarbon reserves. Due to the increasing demand for oil and gas, it is necessary to find new sources of energy to fulfil these energy requirements. The development of these unconventional resources and maximizing production from them will be crucial for energy sustenance in the future.

Unconventional resources are defined as formations that cannot be produced at economic flow-rates or that do not produce economic volumes of oil and gas without stimulation treatments or special recovery processes (Miskimins. 2009). Unconventional resources include tight oil and gas, shale gas, shale oil, coalbed methane, heavy oil/tar sands and methane hydrates. These hydrocarbon reservoirs generally have low-porosity and low-permeability making them difficult to produce. Moreover, there is rapid pressure and production decline making these reservoirs unfavorable candidates for a long-term project. Enhanced oil recovery techniques must be performed to commercially produce these reservoirs making the process more complicated than conventional hydrocarbon resources. Conventional oil and gas resources make up only a third of the total worldwide oil and gas reserves and are fast declining. Figure 1 shows the distribution of hydrocarbon resources in the world. Thus, maximizing recovery from

unconventional resources is an important challenge for the oil and gas industry in the coming decade.

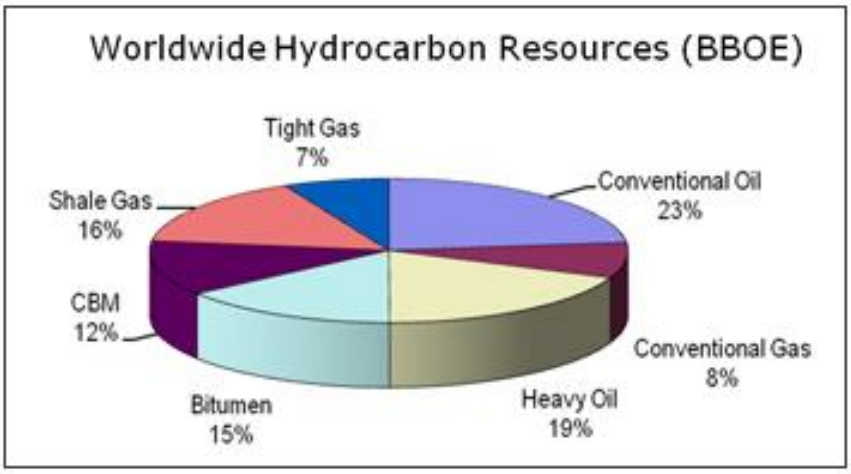

Figure 1: Worldwide hydrocarbon resource distribution (CGG)

1.1 Project Overview

The Granite Wash formation is a tight oil and gas play in the Anadarko basin with varying production trends throughout its extent. It is made up of a series of stacked pay zones which produce competitive rates of gas, light oil and condensates. Two horizontal wells with multi-stage hydraulic fractures have been drilled in the Missourian Wash series in this formation with high initial oil rates. As seen in many tight reservoirs, production declines rapidly and the Gas-Oil ratio (GOR) increases significantly in both the wells. Using reservoir and fluid analysis data, we test the efficacy of enhanced oil recovery techniques in this field.

1.2 Research Objectives

- Conduct detailed geologic modeling using well-logs to estimate porosity, saturation and shale content
- Analyze Diagnostic Fracture Injection Test (DFIT) report & microseimic fracture maps to characterize reservoir properties & understand completion efficiency respectively
- Using PVT reports, accurately model laboratory experiments in a phase behaviour & fluid property software module to predict fluid behaviour in depletion scenarios
- Develop a reservoir simulation model to match historical production data and test the field response to water injection

1.3 Thesis Outline

The contents of each chapter are summarized below.

Chapter I is brief introduction to the research topic, project overview and its objectives. Chapter II is a literature review about the petroleum engineering apsects covered in the thesis. This includes tight oil reservoir description, horizontal well technology, hydraulic fracturing and multi-stage fracturing processes, waterflooding & microseismic fracture monitoring.

Chapter III decsibes the Anadarko basin stratigraphy, and then discusses the Granite Wash formation geological characteristics. The Missourian Wash series is described in detail and completion trends in the formation are discussed. Chapter IV describes the

petrophysical analysis conducted and the reservoir properties estimated from the study. Chapter V gives a brief description of the Diagnostic Fracture Injection testing method and discusses the results obtained from the claibration test analysis. Chapter VI analyzes the microseismic fracture mapping report and describes the hydraulic fracture characteristics interpreted.

Chapter VII describes the reservoir model setup and sensitivity analysis studies. History matching process and validation of symmetry model is described as well. Chapter VIII describes the waterflooding plans implemented and the results obtained. Chapter IX reports the conclusions obtained and provides recommendations for future work.

CHAPTER II

LITERATURE REVIEW

As discussed in the introductory chapter, only a third of worldwide oil and gas reserves are conventional, and the remainder are unconventional resources. Advanced techniques are required to exploit such types of reservoirs economically because of characteristics such as low porosity, low permeability, high viscosity etc. The resource triangle in Figure 2 helps in visualizing the nature of the resource base.

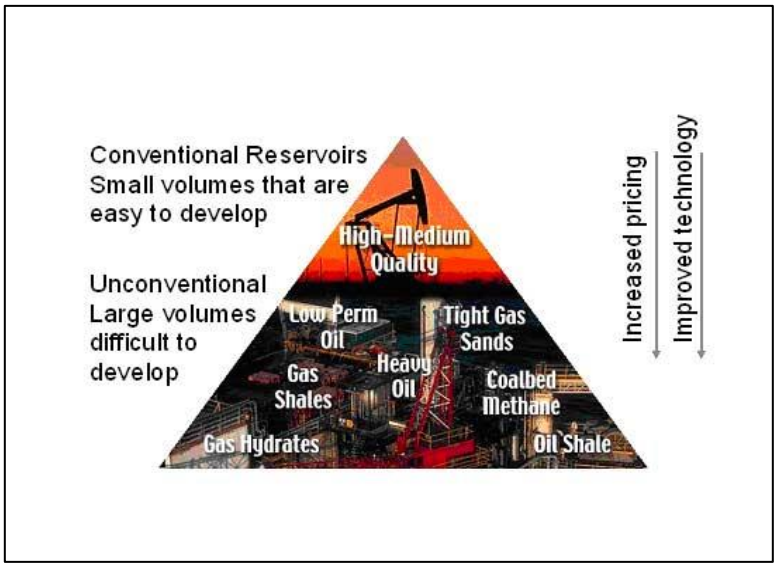

Figure 2: Unconventional resources triangle (Holditch. 2006)

To make unconventional resources flow commercially, unconventional techniques in exploration, drilling, completions and characterization are required. The oil and gas

industry has focused its research efforts on maximizing recovery from these resources which will help meet the energy demands in the coming decades.

2.1 Tight Oil

Hydrocarbon flow from reservoirs depends on a lot of parameters of which pore size and interconnected pores are of major importance significance. Oil & gas require a conductive pathway to flow from the matrix into the wellbore. In tight reservoirs, producing oil and gas is more difficult than in conventional reservoirs due to relatively small pore size of reservoir rock, lack of interconnected pores & complicated inter-fluid interactions. In conventional reservoirs, the percentage of pore space within the rock volume is less than 30% and in tight oil fields it is generally less than 10%. Figure 3 shows a conventional sandstone cross-section, while figure 4 shows a tight-sand cross-section. The term “tight oil” is used for oil produced from reservoirs with relatively low porosity and permeability (Naik. 2003).

The term “tight oil” has been used for a wide variety of reservoir conditions which differ from area to area. Tight oil reservoirs are known as “continuous” resources as they tend to spread over large areas without significant downdip water accumulation unlike conventional oil reservoirs (Anonymous). A lot of untapped reserves are left in these reservoirs due to their varying nature.

There are two main types of tight oil:

• Oil present in source-rocks such as shale. This kind of reservoir is characterized by very low reservoir quality and production using conventional techniques is impractical. The latest technological advances are required to make these reservoirs flow.

• Oil migrated from original shale source rock and accumulated in nearby or distant tight sandstones, siltstones, limestones or dolostones. This kind of tight oil rocks usually have better quality than shales with larger porosity, but still lower quality than conventional reservoir. Figure 4 shows a similar tight sand cross-section.

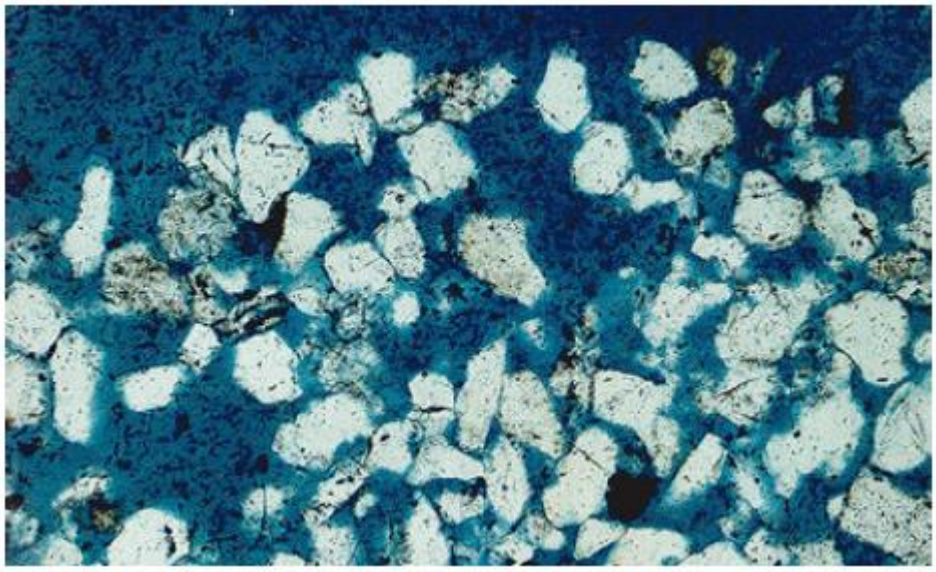

Figure 3: Conventional sandstone cross-section (Naik. 2003)

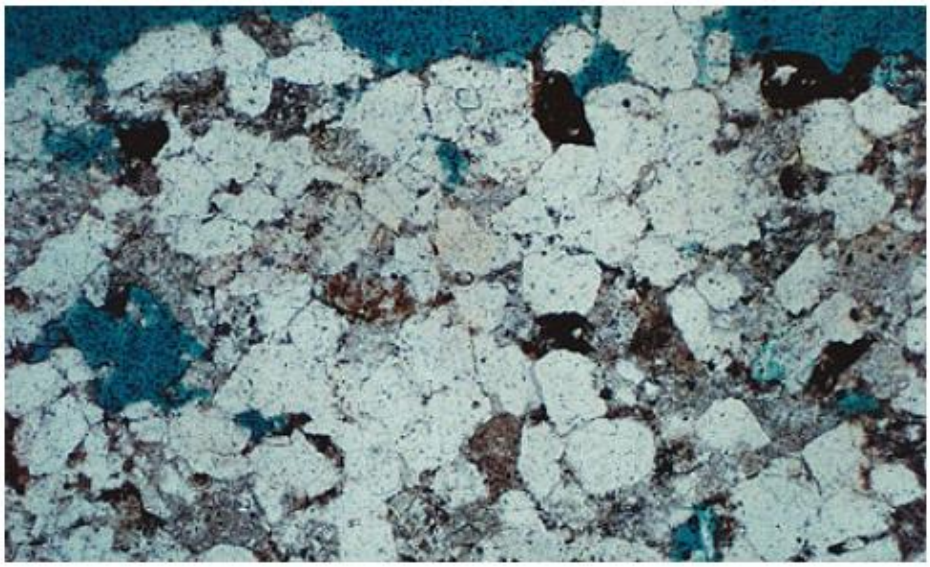

Figure 4: Tight sand cross-section (Naik. 2003)

Tight oil reservoirs use the same technologies for stimulation as shale gas plays, and tight oil and gas can be found in the same reservoir in some cases. The unconventional boom occurring now can double the economic benefits experienced on the gas side. A lot of new as well as mature tight oil and liquid-rich plays have been made profitable by horizontal drilling and multistage completion. To date, the industry has identified about 50 billion barrels of oil equivalent recoverable reserves from tight U.S. plays. In figure, current and prospective tight, fine-grained oil plays are shown. Figure 5 shows the tight-oil resource play in United States of America.

Figure 5: Tight oil plays in USA (IHS)

2.2 Horizontal Well Technology

In the last decades, the applications of horizontal well technology have been widely facilitated by the surging of unconventional reservoirs. At a low drawdown, a horizontal well can have a larger productivity in comparison with vertical wells. The major advantage of horizontal well technology is to enhance the contact area with the formation.

Now it is well understood that horizontal well is one of the greatest improvements in economically developing tight gas and oil reservoirs. The increasing oil price along with the advancements in horizontal drilling and hydraulic fracturing technologies have allowed industries to meet the future energy demand although in the facing of rapid decline in tradition hydrocarbon reserves. The advantages of horizontal well can be considered as followings:

1. Increased production rate because of the greater wellbore length exposed to the pay zone
2. Reduced possibility of water or gas cresting
3. Use in enhanced recovery applications
4. Larger and more efficient drainage pattern leading to increased overall reserves recovery
5. Cross several interested pay zones

2.3 Hydraulic Fracturing

The ability of hydrocarbons to flow from the reservoir depends on permeability which represents the interconnected pores in the rock. In order to produce oil and gas from low-permeability reservoirs, a conductive path needs to be created with a pressure difference so hydrocarbons are displaced. Hydraulic fracturing is a technique to artificially stimulate low-permeability formations in order to extract oil and gas trapped underground. This is achieved by pumping fracturing fluid under high pressures to induce cracks in the formation. The fissures created are help open by sand particles to provide inroads for oil and gas into the wellbore.

Figure 6 shows a conventional vertical well without a stimulation job where the arrows represent the flow of fluid into the wellbore. In the lower part, the same well with fractures is seen and hydrocarbons flow from the matrix into the fractures and subsequently to the wellbore. Hydraulic fracturing improves the exposed area of the pay

zone and creates a high permeability path which extends significantly from the wellbore to a target production formation. Hence, reservoir fluid can flow more easily from the formation to the wellbore (Holditch. 2006). Figure 6 compares natural completion & hydraulic fracture completion.

During hydraulic fracture, fluids, commonly made up of water and chemical additives, are pumped into the production casing, through the perforations, and into the targeted formation at pressures high enough to cause the rock within the targeted formation to fracture. When the pressure exceeds the rock strength, the fluids open or enlarge fractures that can extend several hundred feet away from the well. After the fractures are created, a propping agent is pumped into the fractures to keep them from closing when the pumping pressure is released. After fracturing is completed, the internal pressure of the geologic formation cause the injected fracturing fluids to rise to the surface where it may be stored in tanks or pits prior to disposal or recycling (EPA webpage).

Recovered fracturing fluids are referred to as flow-back. Disposal options for flow-back include discharge into surface water or underground injection. Well fracturing technology can improve the fluid flow in low permeability, heterogeneity, thin reservoir and reservoir with poor connectivity, it can increase the production of single well and the ultimate recovery factor (Cooke Jr. 2005).

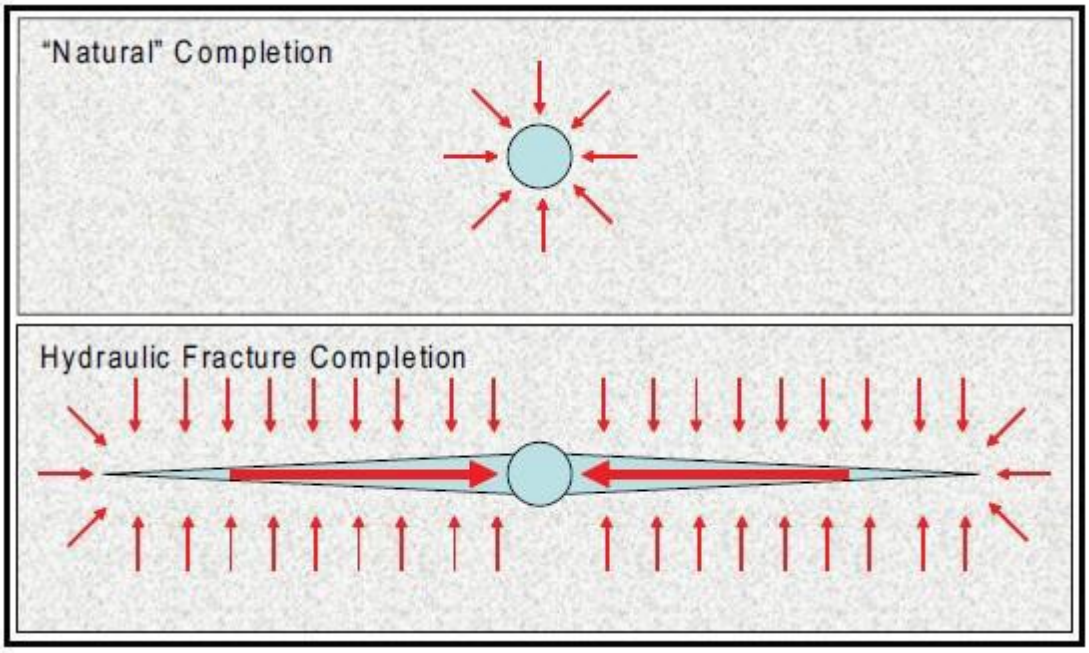

Figure 6: Hydraulic fracturing process

2.4 Horizontal Well with Multi-stage Hydraulic Fracturing

Advanced stimulation and completion technology is needed to commercially produce tight oil and gas reservoirs. Maximizing the total stimulated reservoir volume is extremely important in successful oil production. The growth in multi-stage fracturing has been tremendous over the last four years due to completion technology that can effectively place fractures in specific places in the wellbore. By placing the fracture in specific places in the horizontal wellbore, there is a greater chance to increase the cumulative production in a shorter time frame (Song et al. 2011). Every fracturing stage is separated from the next one using ball and packer seals, and fracturing fluid in injected to crack the formation. These highly conductive multiple fractures pull in

hydrocarbons from the surrounding matrix. Figure 7 shows the multi-stage fracturing process.

Figure 7: Multi-stage hydraulic fracturing (FracStim)

The main advantages of multi-stage hydraulic fracturing include incremental recovery of the resource, reduced number wells required to be drilled resulting in less construction time and the ability to precisely fracture intended formation zone. The combination of horizontal drilling and multistage hydraulic fracturing technology has made possible the current flourishing gas & oil production from tight reservoirs in the United States.

2.5 Flow Patterns in Hydraulically Fractured Wells

Five distinct flow patterns occur in the fracture and formation around a hydraulically fractured well. Successive flow patterns often are separated by transition periods including fracture linear, bilinear, formation linear, elliptical, and pseudoradial flow. But the fracture linear flow period which lasts very short time and may be masked by wellbore storage effects (Petrowiki). In the linear flow, most of the flow liquid comes

from the expansion of liquid in the fracture which is similar to the flow occurring in wellbore storage. Interpreting the pressure transient data in hydraulically fractured wells is important in evaluating the success of fracture treatment and for predicting fracture performance of fractured wells. Figure 8 shows the different types of flow patterns in a fractured well.

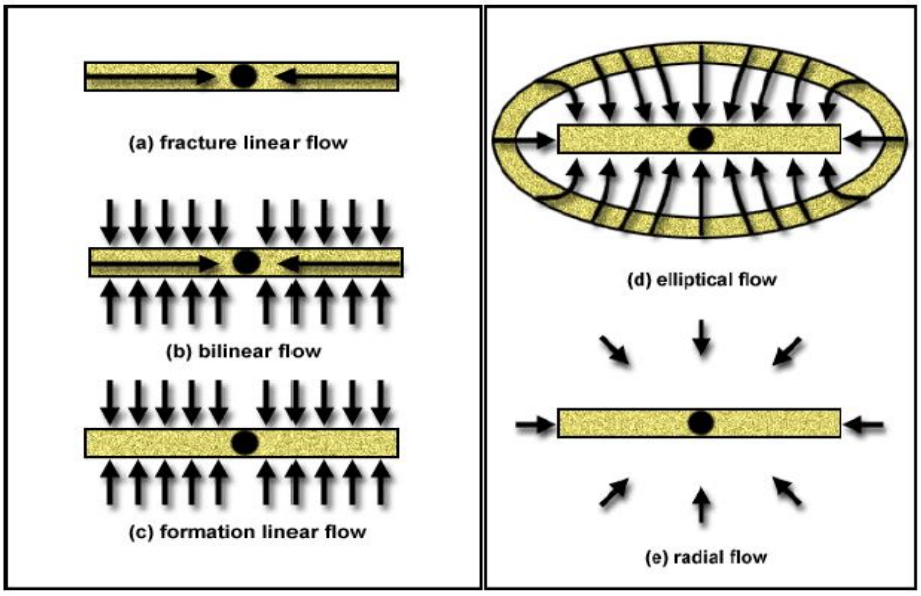

Figure 8: Types of flow in fractured horizontal well

2.6 Water Injection

Water flooding is an enhanced oil recovery process in which injected water is used to displace remaining oil after primary recovery. Water is injected into a reservoir through injection wells to initiate a sweep mechanism that drives the reservoir oil toward the production wells. A bottom water drive is seen as injected water pushes oil upwards

towards the production well. Figure 9 shows waterflooding in vertical wells. In earlier practices, water injection was done in the later phase of the reservoir life but now it is carried out in the earlier phase so that voidage and gas cap in the reservoir are avoided (Gulick and McCain. 1998). Using water injection in earlier phase helps in improving the production as once secondary gas cap is formed the injected water initially tends to compress free gas cap and later on pushes the oil thus the amount of injection water required is much more (Rose et al. 1989).

The water injection is generally carried out when solution gas drive is present or water drive is weak. Therefore for better economy the water injection is carried out when the reservoir pressure is higher than the saturation pressure (Jelmert, 2010).

Water is injected for two reasons:

- For pressure support of the reservoir.
- To sweep or displace the oil from the reservoir, and push it towards an oil production well.

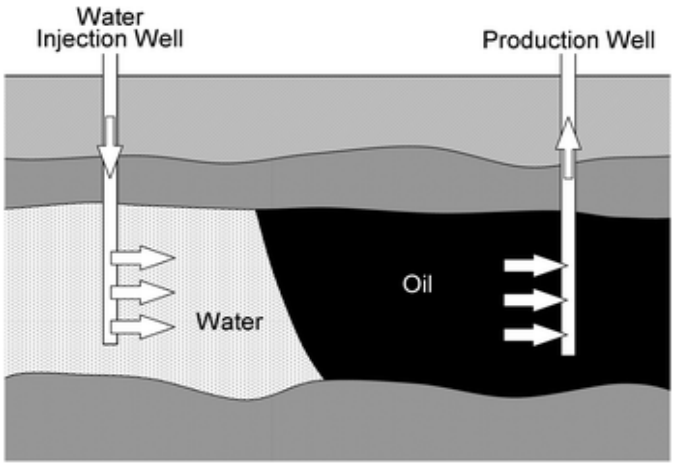

Figure 9: Standard waterflood schematic (Shah et al. 2010)

2.7 Microseismic Monitoring

Microseismic monitoring is an important tool for imaging fracture networks & optimizing completion procedures. It helps detect the fracture complexity resulting from injections in a reservoir. Basically, microseismic monitoring is the placement of receiver systems in close locations by which small earthquakes (microseisms) induced by the fracturing process can be detected & located to provide fracture propagation information (Warpinski. 2009) . Figure 10 shows a microseismic event cloud.

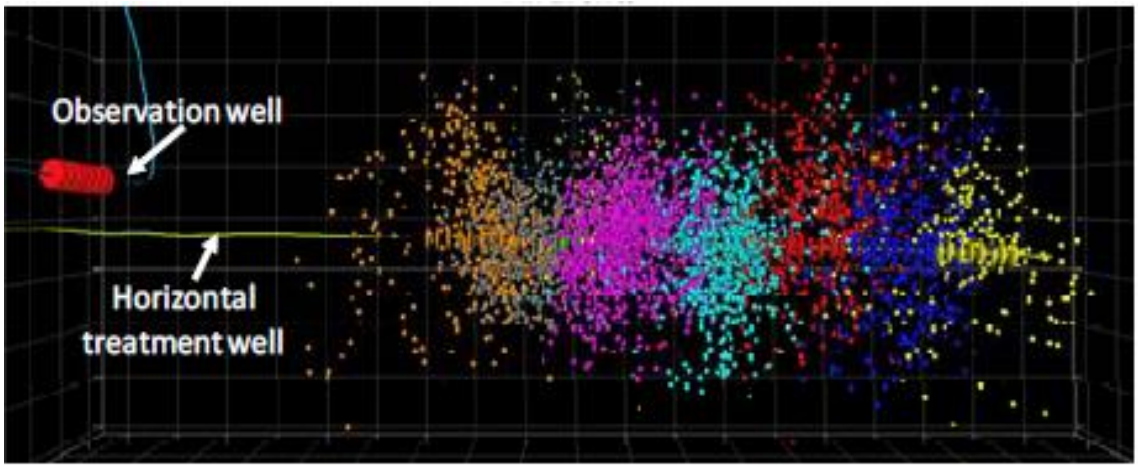

Figure 10: Microseismic monitoring schematic (Maxwell, 2011)

The primary information about the hydraulic fractures comes from the locations on the microseismic clouds. The positioning of the receiver system is critical in obtaining a good signal to noise ratio. The best vertical position is to have the array straddling the fracture zone (Warpinski. 2009). Noise issues are a problem in micorseismic monitoring. As microseismic events generate very weak signals, a relatively small amount of noise

can ruin the mapping exercise. The most important issue in micorseimic monitoring is the uncertainty of event locations(Maxwell et al. 2008). There is uncertainty in the data, and also in the velocity models which further complicates the issue. As microseisms begin to spread away from the perforations, they begin to collect velocity-related errors. Near events are not affected in a major way but far events have large uncertainties in their positioning. Observation well bias occurs in measurement as events closer to the monitor well are picked up easily but those arther away are not recorded. Possible assymetry can be seen due to this which hampers fracture interpretation. The intensity of micorseisms depends on parameters such as fluid injection rate and volume as they control the amount of energy put into the formation.

Proper interpretaion of recorded data is very necessary as well. Micoseisms are not just points of failure at the fracture tip, they can be either shear or tensile events that occur around natural fractures present or points of weakness in the reservoir(Warpinski.). They are small shear slippages that are induced by change in stress & pressure caused by the injection process. This results in a hazy interpreation about the hydraulic fracture network. If the microseisms are generated only as a result of stress changes induced by hydraulic fractures, then a scctter of microseisms should be generated only along the fractre length on both sides of the perforation. Though, this is never the case in reality. Especially in oil reservoirs, due to relative incompressibility of the fluid, pressure can be coupled large distances leading to a wider scatter of the microseisms(Warpinski. 2009). It is particularly helpful if linear fractures can be determined to assist in interpretation.

CHAPTER III

GRANITE WASH PLAY

The Granite Wash reservoirs are part of the Anadarko Basin play extending across Texas & Oklahoma. There has been major activity in this area since the Elk City field was discovered in Beckham County in 1947. Reservoir depths range from 8,000 to 16,000 ft consisting of series of tight oil/gas stacked pays. These series of reservoirs include arkosic sandstones, boulder-bearing conglomerates and carbonate wash, all of which is conveniently labeled as "Granite Wash" (Mitchell. 2011). The rocks vary from being quartz and feldspar rich at the top and more finely grained and carbonite resembling down section.

3.1 Geologic Setting

The erosion of earlier Precambriam basement atop the Amarillo-Wichita Uplift resulted in the deposition of fine to course-grained, poorly sorted sandstones and carbonaceous clastics in the north of the Uplift. These sediments were deposited as a series of fan-delta, stacked, slope and submarine fan channel deposits (Rothkopf et al. 2011). Several trapping mechanisms such as stratigraphic overlaps, folds, faults & large scale unconformities have provided favorable conditions for hydrocarbon deposition (Srinivasan et al. 2011). The strike of the Granite Wash Reservoirs is northwest-southeast which is parallel to the Amarillo-Wichita uplift. Many depositional settings

have been suggested for the different reservoirs in Granite Wash. They include fan-delta, turbidite and debris flow environments. Figure 11 shows the cross-section while figure 12 shows the deposition model. A variety of oil and gas traps are present in the area but most traps can be explained as structural and stratigraphic in nature.

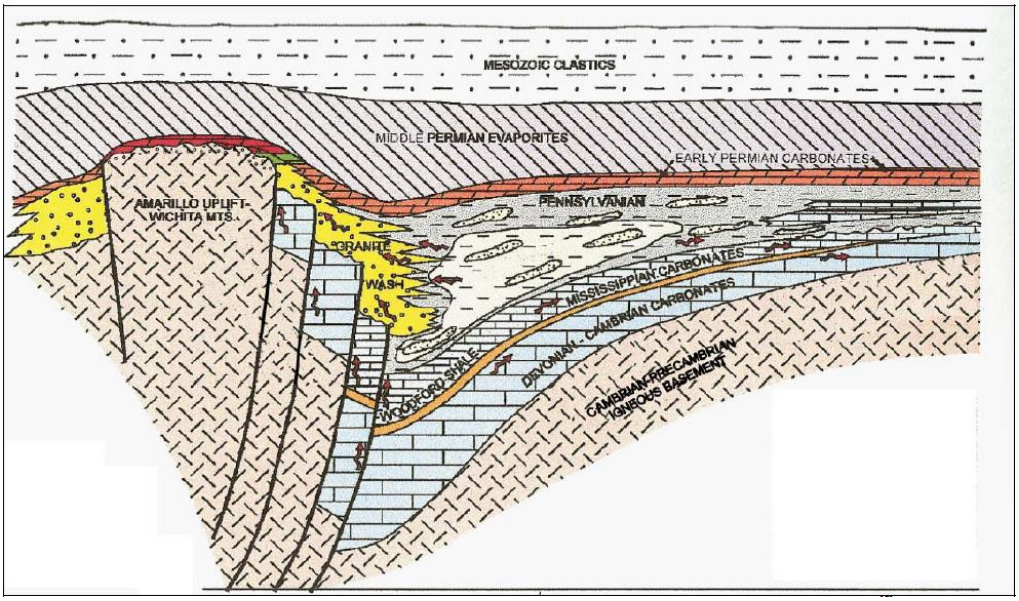

Figure 11: Anadarko basin stratigraphic cross-section (Srinivasan et al. 2011)

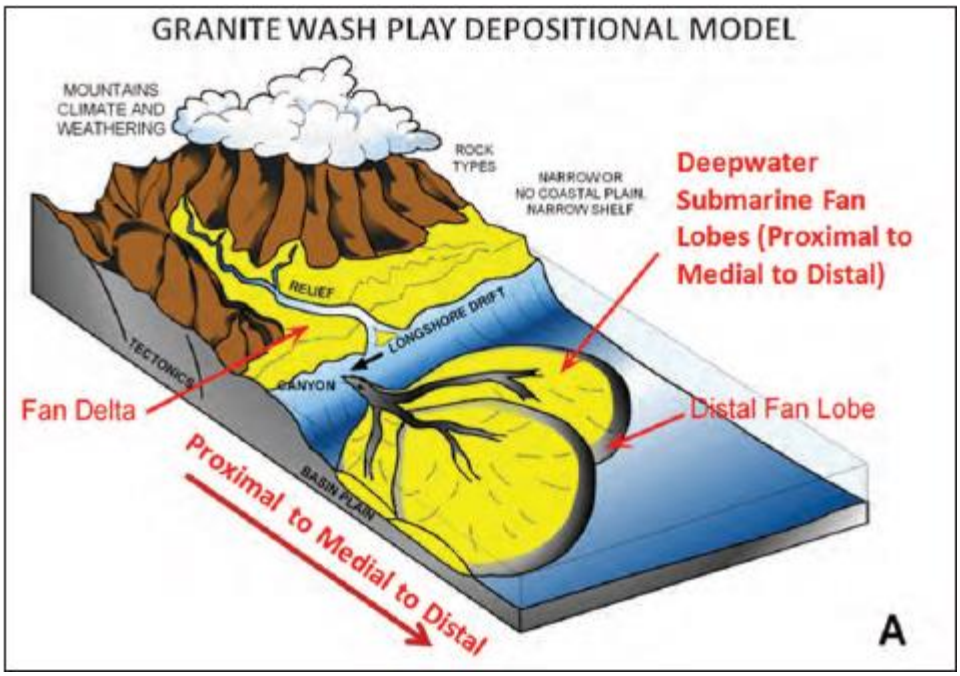

Figure 12: Granite Wash deposition model

3.2 Mineralogy

The production trend is determined by the presence of arkosic sandstone and conglomerates through Atokan to Virgilian age. These reservoirs were deposited proximal to the Amarillo Wichita uplift. Large volumes of clastic sediments were shed off the uplift and deposited in the rapidly subsidizing Anadarko basin. The lithological components may include granite, cryolite, gabbro, limestone and chert. As for the minerals, the most common is quartz with potassium and sodium feldspars. Other minerals present are calcite, dolomite, illite and chlorite. Figure 13 shows the mineral distribution in Granite Wash play. Due to this complex mineralogy, the grain density has a wide range of values as shown in Figure 14. It varies from 2.57 – 2.69 g/cc depending

upon the reservoir (Smith et al. 2001). Generally 10 to 20 miles from the mountain front, the majority of coarse debris becomes less abundant and the Wash intervals are interbedded with marine shale markers, which are noted on both Desmoinesian and Missourian type logs. (Strickland et al. 2003)

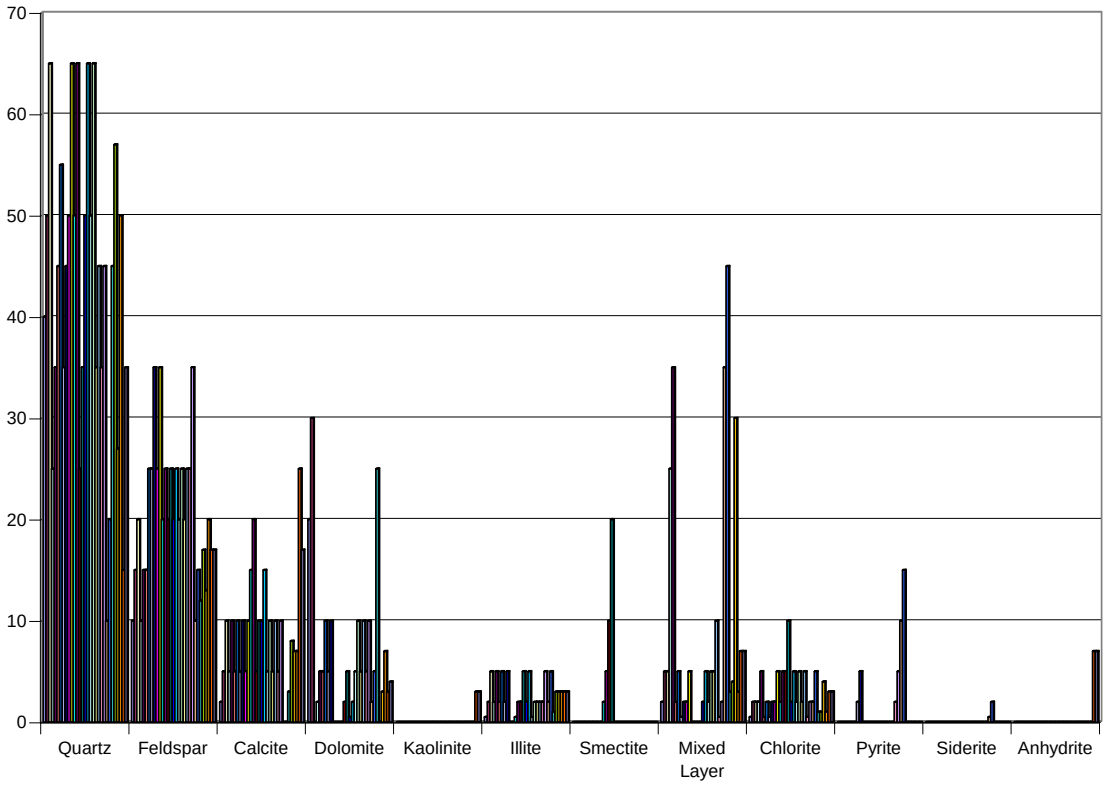

Figure 13: Mineral content of Granite Wash (OGS, 2003)

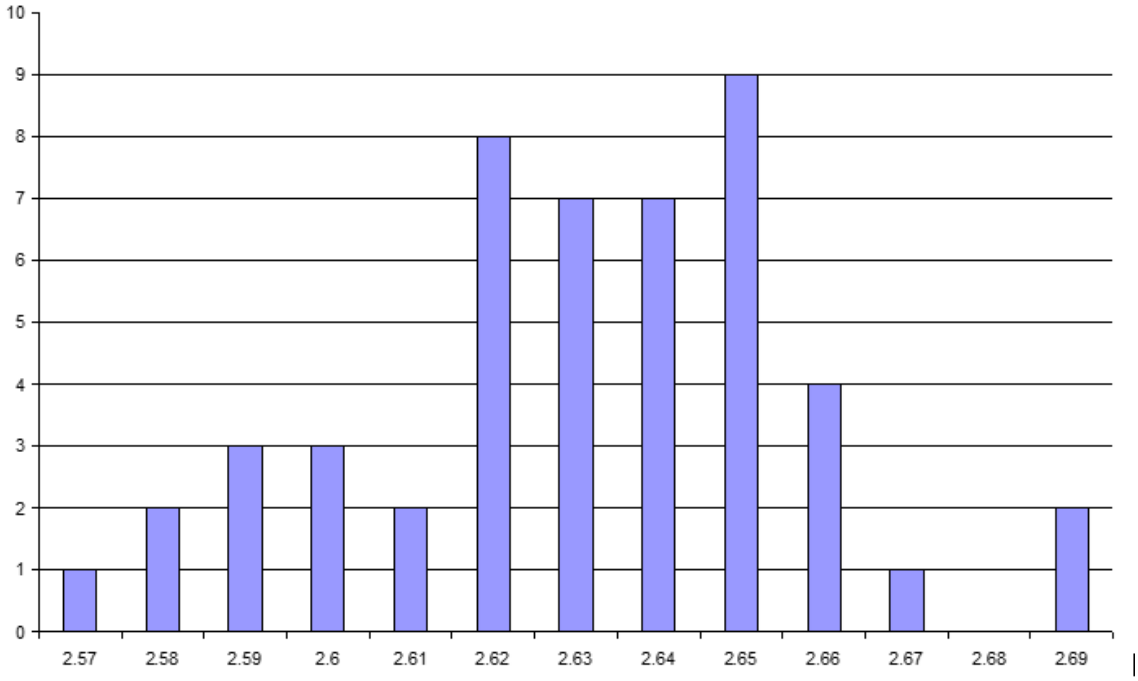

Figure 14: Grain density of Granite Wash (OGS, 2003)

3.3 Hydrocarbon Zones in the Granite Wash

As can be seen from the figure 15, the granite wash consists of stacks of reservoir plays on top of each other. The upper Virgilian and Missourian Wash reservoirs are generally oil prone while the liquid yield becomes progressively leaner as we move towards the Desmoinesian and Atokan reservoirs (Mitchell. 2011). There are a minimum of 14 separate reservoirs in the Granite Wash play. Individual reservoir thickness ranges from 30 to 200 ft. The limited knowledge of reservoir permeability, pressure, porosity and water saturation led to an inferior understanding of the original hydrocarbon in place. The oil and gas ratios vary laterally and vertically due to the inherent heterogeneity of the Granite Wash reservoir.

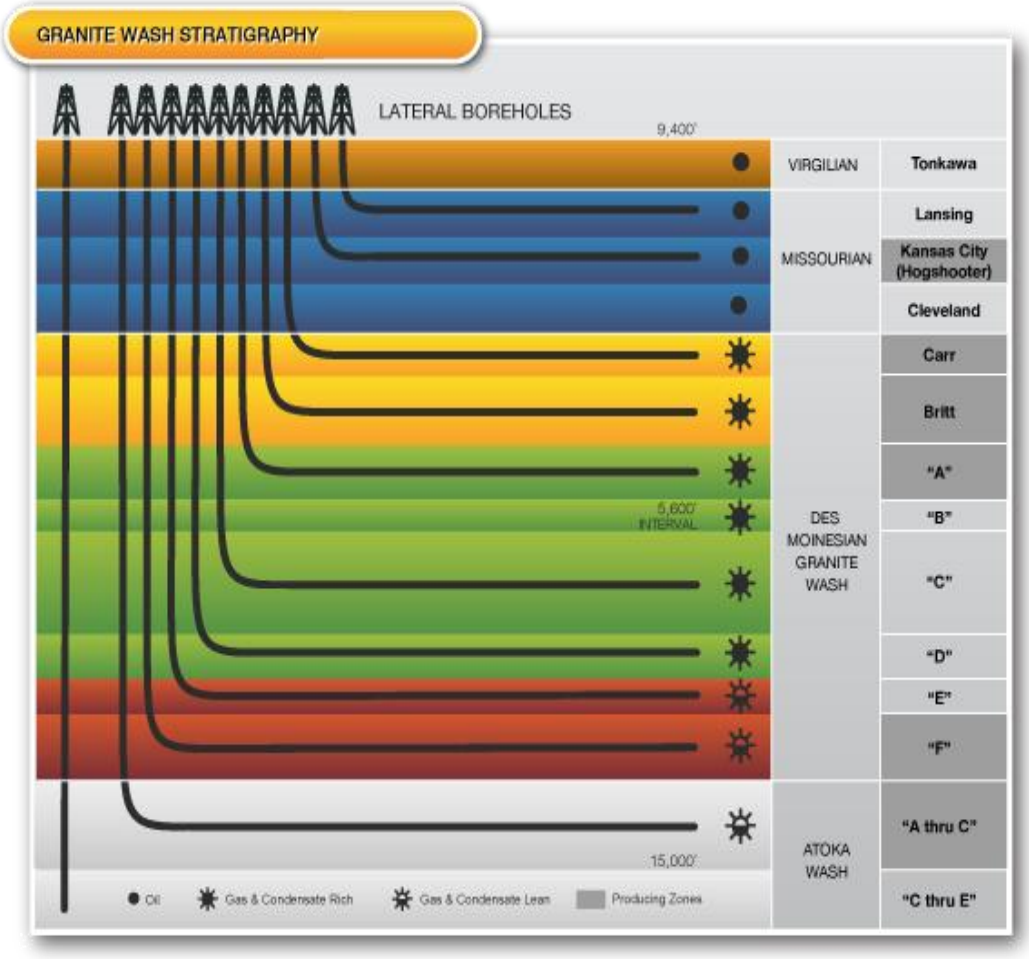

Figure 15: Granite Wash reservoirs and hydrocarbon type (Linn Energy)

3.4 Missourian Series Wash

The Missourian Wash series has three intervals, the Cottage Grove, Hogshooter and Checkerboard washes as shown in figure 16. Each contain a pair of radioactive black-shale beds that extend across the region. The main depositional thickness is immediately adjacent to the uplift and extends westwards into Wheeler County. The earliest oil & gas discovery was made from the Missourian Wash series in 1947 near the Elk City

Anticline in Oklahoma.(Mitchell. 2011) The Missourian series is comprised of arkosic conglomerates and sandstone. The Wheeler county play area offers largest areal extent and selection of horizontal targets. The Hogshooter Wash/ Missourian Wash A, B and C (in operator terminology) are oil-bearing reservoirs that are normally pressured and provide good area for horizontal drilling. Oil gravities range from 42 – 47 API. The Missourian Wash B formation in which the study wells are drilled has a maximum net pay of 50 ft and is separated from the Missourian Wash A & C by 40 – 50 ft. of shale zone. The shale zones make it convenient in locating individual pay zones on well logs.

One of the source rocks for hydrocarbon deposition in the Granite Wash is believed to be the thin radioactive shales in the Missourian section. The Total Organic Content (TOC) of shales in the Missourian section is 2-6% and are well into the oil window (Mitchell, 2011). The conglomerate and Arkosic sandstone secton of the Missourian Wash interval is often calcareous and gradually change into shale and siltstone as we move northwest. There is significant oil potential in this area as horizontal drilling techniques help in accessing relatively thin liquid-rich sections.

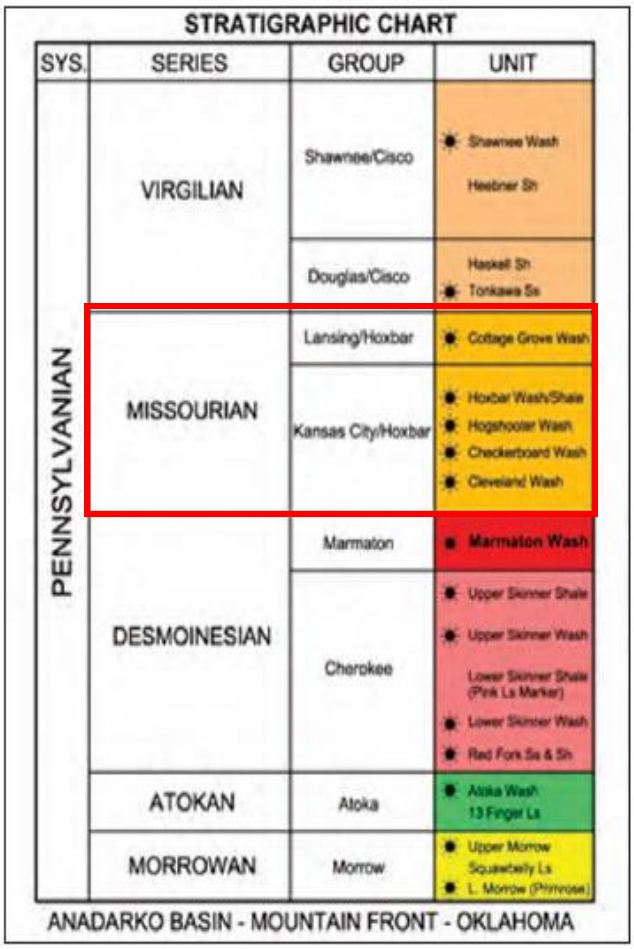

Figure 16: Stratigraphic zonation of Granite Wash highlighting the Missourian Wash series (Mitchell, 2011)

3.5 Granite Wash Completions

Till 2008, vertical completions were the primary method of completion. The vertical methodology complicated efforts to effectively quantify the amount of hydrocarbons as the vertical variations in such reservoirs have made it difficult to ascertain the area drained by the wells. From 2008, operators have been targeting individual zones with horizontal well completions. Wells placed in a 30 -200 ft thick reservoir will generally

drain a more limited vertical well but a larger horizontal area. Better returns on the horizontal wells have all but eliminated the vertical completion option in the area. Figure 17 shows the increasing trend of horizontal drilling in the area.The horizontal drilling permits have substantially risen and the number keeps going higher. Due to high oil price and low natural gas demand, operators are targeting the liquid-rich zones in the Granite Wash.

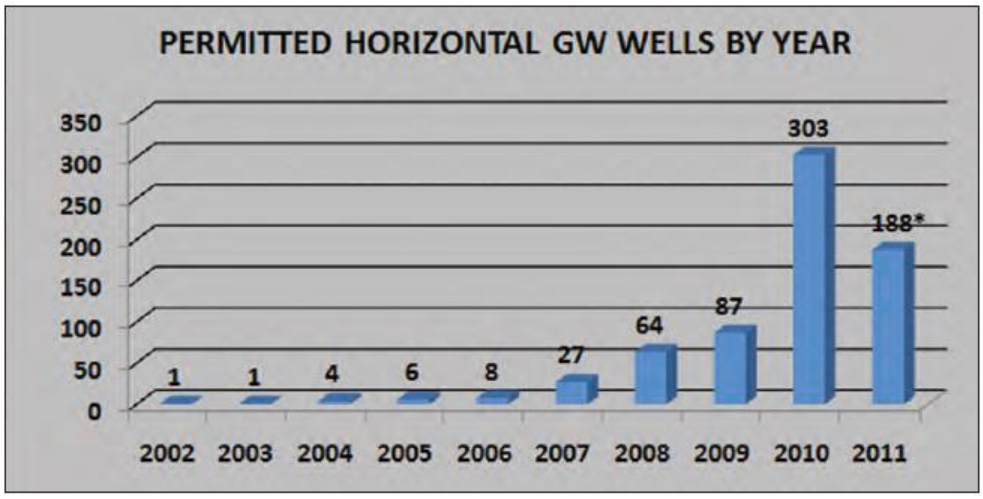

Figure 17: Permitted horizontal wells till first quarter of 2011 (Mitchell, 2011)

The Granite Wash being a tight formation, hydraulic fracturing is essential to makes the wells flow economically. As investigated by Srinivasan et al, lateral well lengths from 3500 to 4500 feet are common in the Granite Wash. Primarily 30/50 & 40/70 white sand proppants are used and in some cases resin coated proppant is injected as a tail-in. Average of 200,00lbs to 250,000lbs proppant volume per stage is common and this

changes according to the reservoir thickness, number of stages & lateral length (Srinivasan et al. 2013).

CHAPTER IV

PETROPHYSICAL ANALYSIS

Data used for the petrophyscial analysis of the Granite Wash field consisted of the well logs runs in the lateral section of Well-1 and some offset vertical wells. A digital log database was developed using Gamma Ray, Spontaneous Potential, Resistivity, Porosity, Sonic and PEF logs. This log suite was interpreted for type of rocks and saturation and porosity estimates were calculated. A simple flowchart explaining the well log analysis is given in figure 18. The marine shale markers are helpful in determining the zone of interest from well logs.

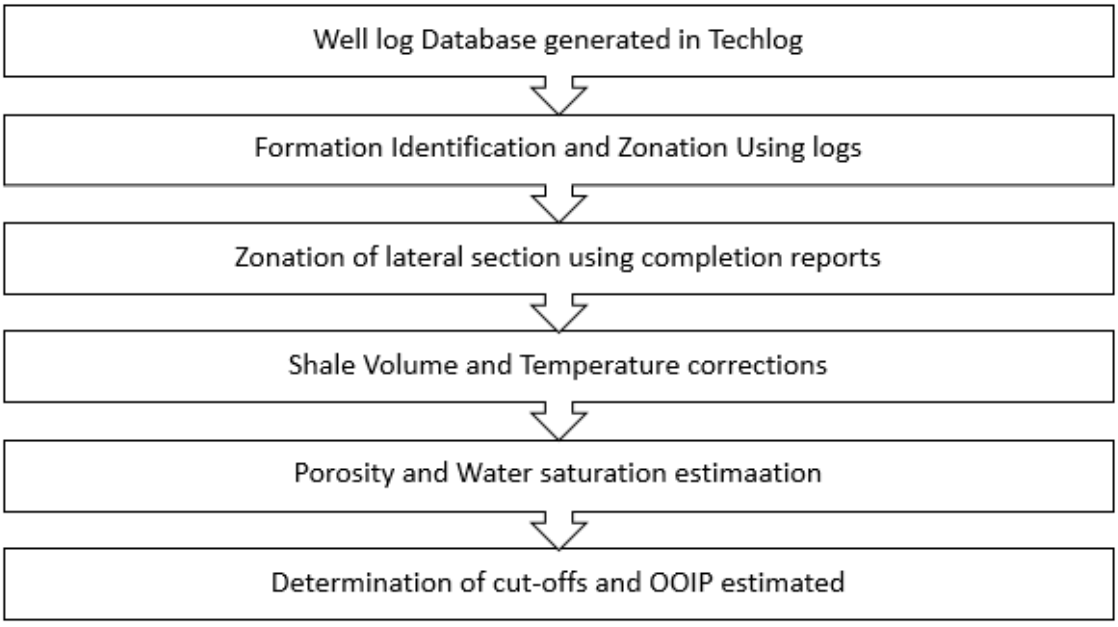

Figure 18: Flowchart showing petrophyscial analysis sequence

As seen in Figure 19, the Missourian Wash B cross-section stratigraphy is shown with the highlighted part showing the net pay close to 50 ft throughout the section. Shale beds are seen above and below the zone of interest indicated by high Gamma-Ray log values.

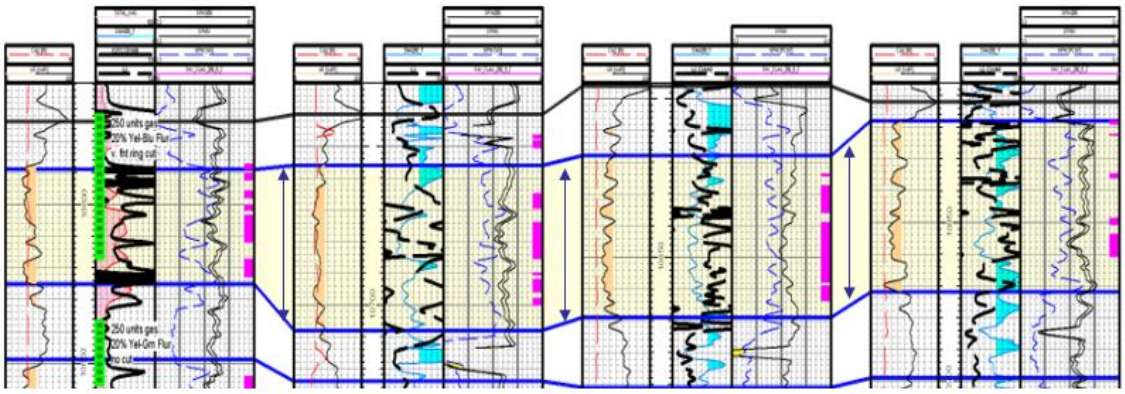

Figure 19: Missourian Wash "B" cross-section stratigraphy across vertical wells in the field (Operator data)

The Granite Wash has significant amounts of clay volume so Shale estimates were calculated using Neutron-Density method (Cairn. 2001). Granite wash formations are moderately radioactive sands due to presence of feldspar which has potassium. Therefore, Gamma Ray values can be confusing in determining sand sequences as the values are inflated. But combining Gamma Ray with resistivity logs helps in resolving the issue of sandstone determination. Resistivity logs show low values in shale zones and a corresponding high value of Gamma Ray indicates a shale zone. Whereas in shaly sand zones, the resistivity plots are higher and Gamma Ray is lower. The matrix density is considered as 2.65g/cc. Figure 20 depicts the logging analysis template in Techlog.

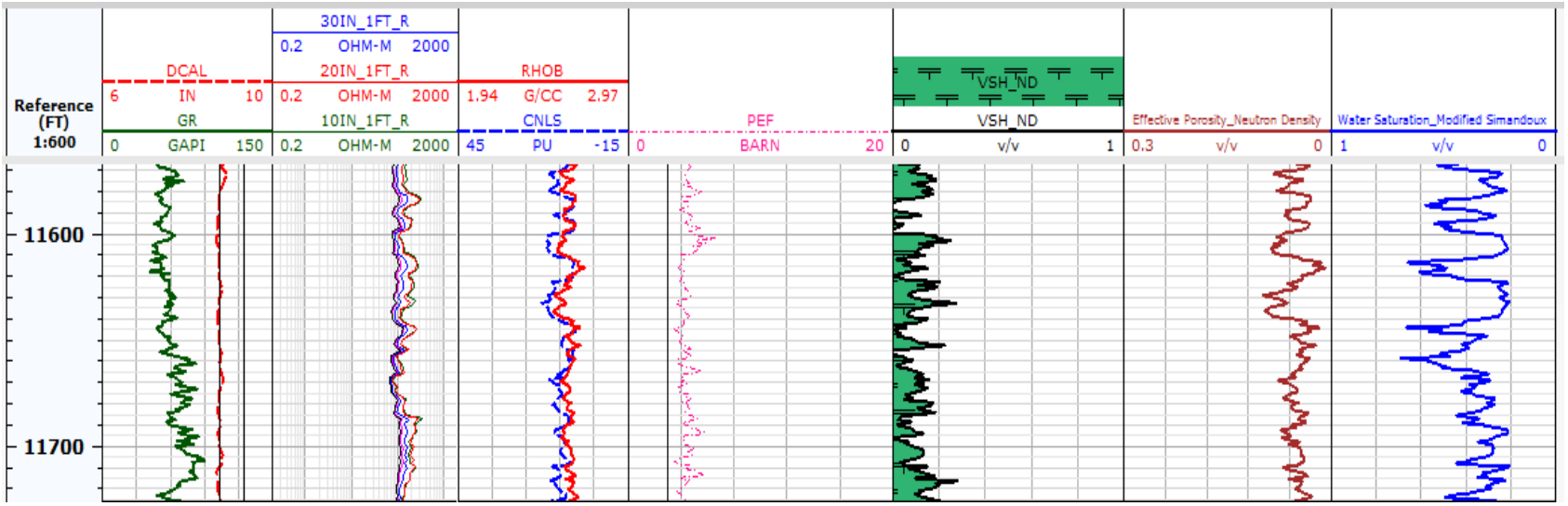

Figure 20: The well-log template of a zone in Well-1 lateral section

4.1 Methodology

The shale volume is calculated using the Neutron-Density model. The inputs used for the analysis are neutron porosity values in the zone of interest, 100% shale, clean sand matrix rock and 100% fluid (water). Similarly, bulk density values in zone of interest, 100% shale, clean sand matrix and 100% water are required. The equations are given by,

$$X1 = NPHI + M \times (RHOB_{MA} - RHOB) \quad \ldots (1)$$

$$X2 = NPHI_{SH} + M \times (RHOB_{MA} - RHOB_{SH}) \quad \ldots (2)$$

$$M = (NPHI_{FL} - NPHI_{MA}) / (RHO_{FL} - RHOB_{MA}) \quad \ldots (3)$$

Using the above equations, shale volume is calculated as

$$Vsh = (X1 - X2) / (X2 - NPHI_{MA}) \quad \ldots (4)$$

Neutron curve values of 0.03 was used for clean formation and 0.37 for clay zone. Porosity was calculated using log measurements of Neutron and Density porosities. The neutron and density porosities were corrected for shale volume. The formula used is,

$$PHID_{CR} = PHID - Vsh * PHID_{SH} \quad \ldots (5)$$

$$PHIN_{CR} = PHIN - Vsh * PHIN_{SH} \quad \ldots (6)$$

Then effective Porosity is calculated as,

$$\text{PHIE} = \frac{\text{PHIDcr} + \text{PHINcr}}{2}$$

… (7)

The evaluation of water saturation needs a proper evaluation of formation water resistivity. The PVT analysis of reservoir fluid provided a confident value of Rw. During PVT analysis, water samples are analyzed for mineral content analysis and other parameters. Rw was 0.75 ohm at 75°F. Using standard correlations, Rw was calculated at reservoir temperature and then using Arps' equation, water salinity was determined. Arps equation is given as,

$$R_w = \left(0.0123 + \frac{3647.5}{\left[NaCl_{ppm}\right]^{0.955}}\right) \cdot \left(\frac{81.77}{T + 6.77}\right)$$

… (8)

A salinity of close to 20000 ppm was calculated. Considering the high salinity of formation water and the presence of shaly sands, standard Archie's parameters fail in this environment. Therefore, based on offset log analysis and literature review input, Modified Simandoux model was used for calculation of water saturation. Modified Simandoux accounts for the shale content of the rock and generates effective water saturation values. Modified Simandoux model is given by,

$$\frac{1}{R_t} = \frac{\phi_s^m S_{ws}^n}{a \cdot R_w \left(1 - C_{sh}\right)} + \frac{C_{sh} S_{ws}}{R_{sh}}$$

… (9)

The values of exponents used are a = 1, m = 1.94, n = 1.61. The final values of calculated properties is given below in Table 1,

Table 1: Petrophysical Analysis Summary

Well-1 Log Analysis Results	
Average Shale volume	0.24
Average Effective Porosity	0.07
Average Water Saturation	0.29

CHAPTER V

DIAGNOSTIC FRACTURE INJECTION TEST ANALYSIS

In unconventional reservoirs, it is important to obtain a good estimate of formation permeability before any production plan is designed. Moreover, it is important to have fracturing parameters before a stimulation job is performed. A mini-frac or Diagnostic Fracture Injection Test (DFIT) helps in obtaining estimates of leakoff co-efficient, closure pressure, fracture gradient, as well as reservoir parameters such as formation permeability and pressure. In tight formations such as Granite Wash, estimation of formation permeability and pressure by conventional pressure buildup tests can be impractical. This is where the continued acquisition of the injection falloff transient pressures after fracture closure as in the DFIT has provided estimates for formation permeability and pressure (Marongiu Porcu et al. 2014).

5.1 Methodology

While performit a DFIT, a small interval usually at the toe of the lateral section is perforated. High-resolution surface gauges are installed on the wellhead with 1- psi resolution or less and data is recorded in one to two seconds intervals for first day and extended thereafter for longer tests (Nojabaei and Kabir. 2012). Initially, the hole is loaded with water. A surface pump injects water and the wellbore fluid is subjected to

compression. Pressure recording is strated proir to pumping and ends after the falloff is complete.

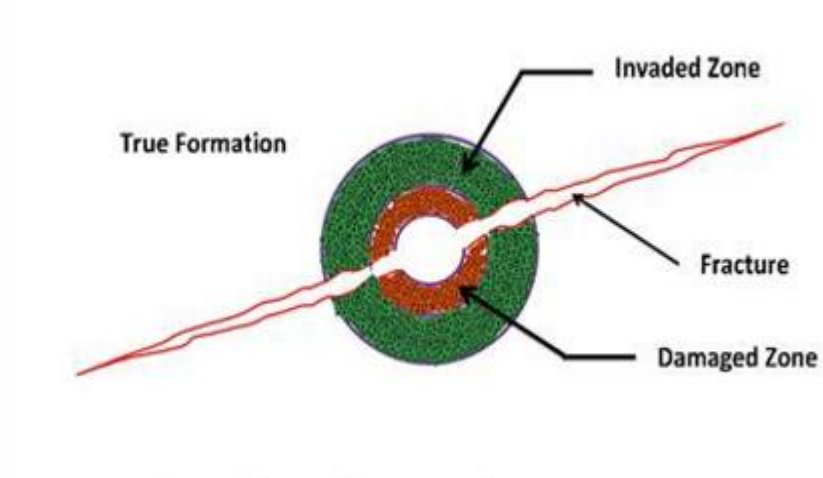

Figure 21: The induced fracture bypasses near well-bore damage and connects to the reservoir interval (Fekete, 2011)

The injection pressure should be high enough to initiate a breakdown in the perforations and create a fracture that passes the invaded zone. Figure 21 shows the process. Eventually, breakdown pressure is reached which signifies a hydraulic fracture is being formed. The water injection is continued till the wellhead pressure stabilizes. After surface injection is stopped, an instantaneous shut-in pressure (ISIP) is recorded. The ISIP is the difference between the final flow pressure and the friction component of the bottomhole calculation. The fracture gradient is obtained by

$$\text{Fracture Gradient (FG)} = \frac{(\text{ISIP} + \text{Hydrostatic Head})}{\text{Depth}}$$

In the above equation, ISIP and Hydrostatic Head are in psi and depth is in ft. The shut-in pressure is then analyzed for fracture closure which is considered equivalent to the minimum principal stress (Nguyen and Cramer. 2013). The after-closure time is evaluated for signs of pseudo- linear and pseudo-radial flow patterns and transient radial flow solution methods are used to estimate reservoir pressure and transmissibility (kh/μ).

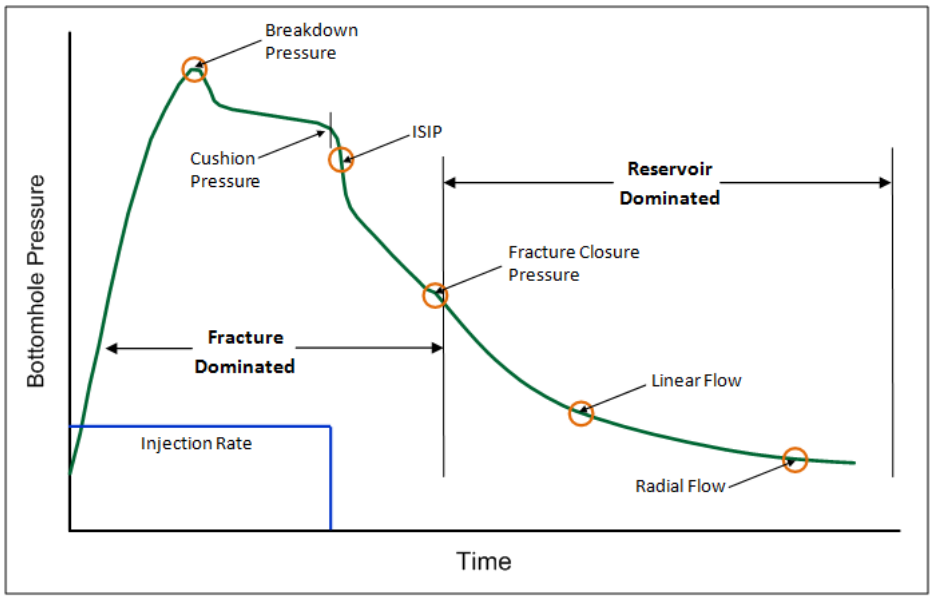

Figure 22: Typical DFIT pressure response (Fekete, 2011)

5.2 DFIT Report Analysis and Results

A DFIT report was obtained from the operator which estimated the formation parameters using standard transient analysis procedures. The water injection was carried out at 4 barrels per minute. It should be noted that proppants are not utilized in a DFIT as

fracture closure analysis is an important aspect to be studied. An Instantaneoous Shut-In Pressure of 3220 psi was recorded during the test as seen in figure 23. Figure shows the casing pressure and slurry rate trends during the injection phase and the ISIP estimate. This corresponds to a fracture gradient of 0.73 psi/ft. This value is useful while determining maximum injection pressure during waterflooding as water has to be injected below formation fracturing pressure.

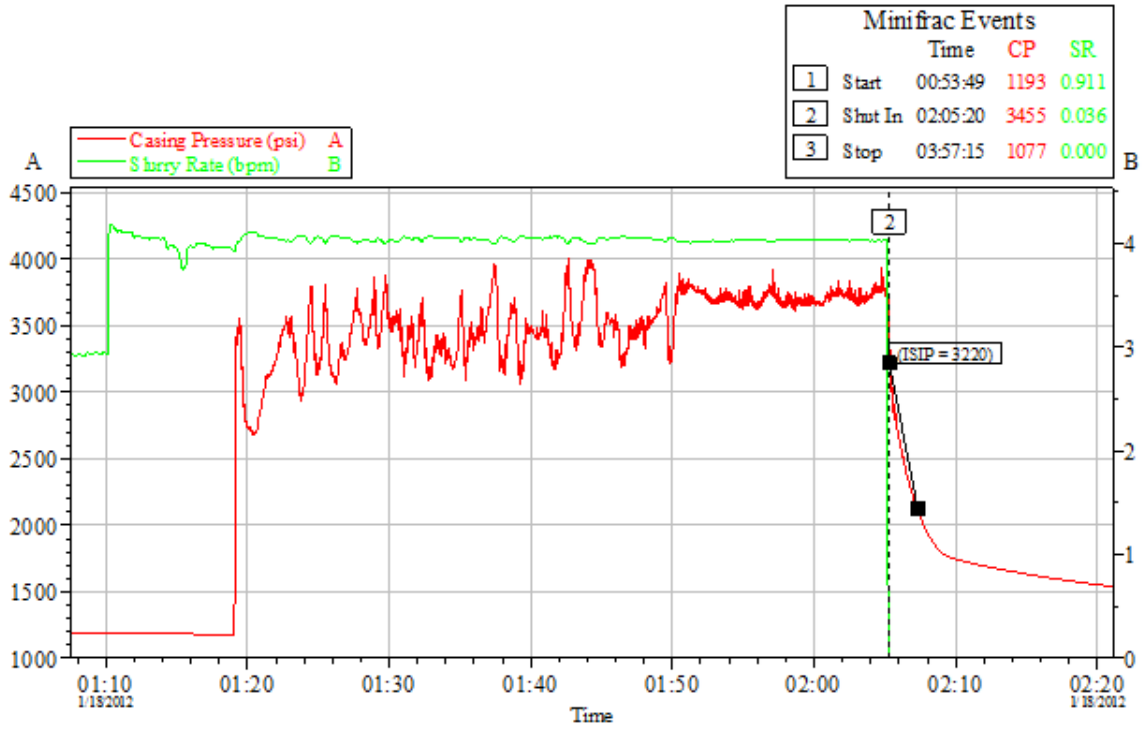

Figure 23: Casing pressure and slurry rate and eventual fall-off plotted against time (DFIT report)

According to the report, a pseudo-radial flow pattern is observed in the fall-off behaviour after approximately 28.94 hours. Using the plot for radial flow time function versus pressure, a transmissibility estimate is determined. The equations used for the analysis are

$$(h) \qquad \frac{4\ (r\ )}{s\ r(\ )} = \frac{}{4\pi*k*h*Tc} \qquad \ldots (10)$$

Above equation can be re-written as,

$$\frac{k\ h}{} = \frac{}{16\ (r\ )\ T\ c} \qquad \ldots (11)$$

Reservoir fluid is assumed to be gas and viscosity is 0.0256 cp. The radial flow time function versus pressure graph as shown in figure estimates the transmissibility to be 84.399 md*ft/cp as seen in figure 24. The net pay of the Missourian Wash B formation is 50 ft, so the permeability yielded is 0.043 md.

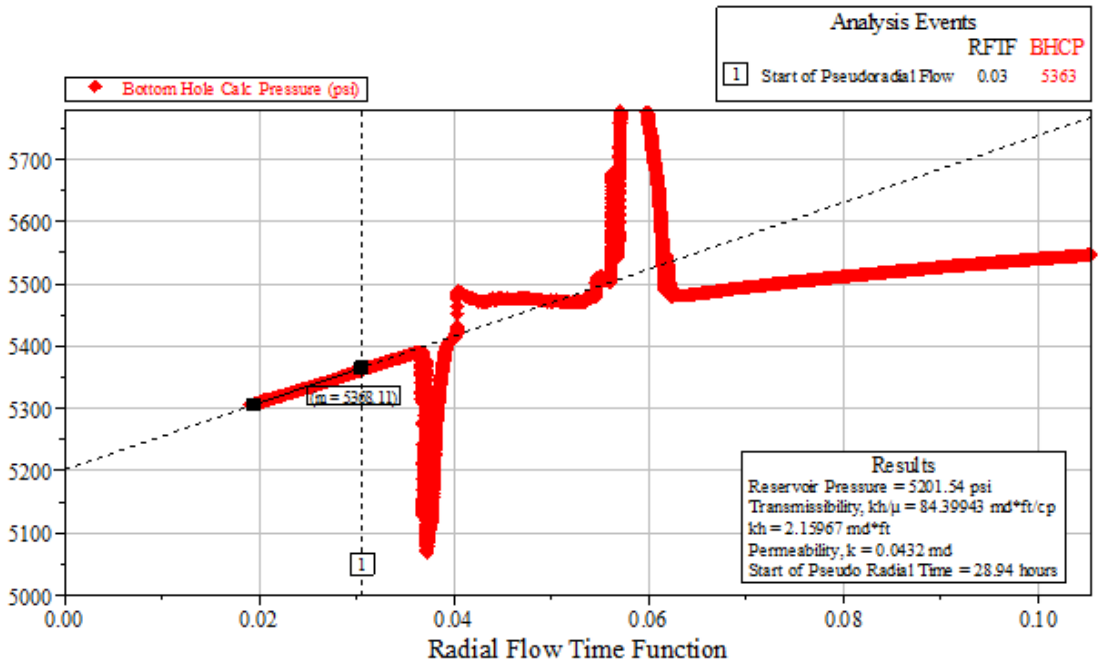

Figure 24: After closure analysis - Cartesian pseudoradial plot (DFIT report, 2011)

The formation permeability estimate obtianed from the DFIT is used as a reference point in our further simulation work. As with any interpretive test, the parameters obtained are susceptible to variation and the values obtained are only as good as the confidence of the interpretation. The permeability obtained from the test is reflective of the tight nature of the Granite wash formation and is carried forward in the simulation studies.

CHAPTER VI

MICROSEISMIC MONITORING REPORT ANALYSIS

Microseismic monitoring is an important tool for imaging fracture networks & optimizing completion procedures. It helps detect the fracture complexity resulting from the injections in a reservoir. Basically, microseismic monitoring is the placement of receiver systems in close locations by which small earthquakes (microseisms) induced by the fracturing process can be detected & located to provide fracture propagation information (Warpinski. 2009). Theses are also critical in enabling fracture optimization by comparing results of different strategies.

6.1 Microseismic Fracture Map Analysis and Discussion

Microseismic analysis was performed on Well-1 and Figure 25 and 26 show the microseismic activity detection around the lateral wellbore. The azimuth appears to be East-West i.e. transverse to current North-South direction of lateral, confirming in-situ stress directions in the area. Fracture height is contained within the target Missourian wash "B". Moderate to complex fracture geometry is observed, with noticeable observation well bias. As a single vertical well in the east direction was used for monitoring, the microseismic events on the west side are too far-off to be detected leading to an asymmetrical microseismic map.

A wide dispersing of events is seen on the fracture map. As explained by Warpinski, pressure response is scattered widely especially in oil reservoirs. Moreover, the propagating hydraulic fracture interacts with pre-existing natural fractures and planes of weaknesses which generate tensile and shear failures. These events are picked up by the receivers as well. Pressure is coupled over long distances leading to a wider scatter.

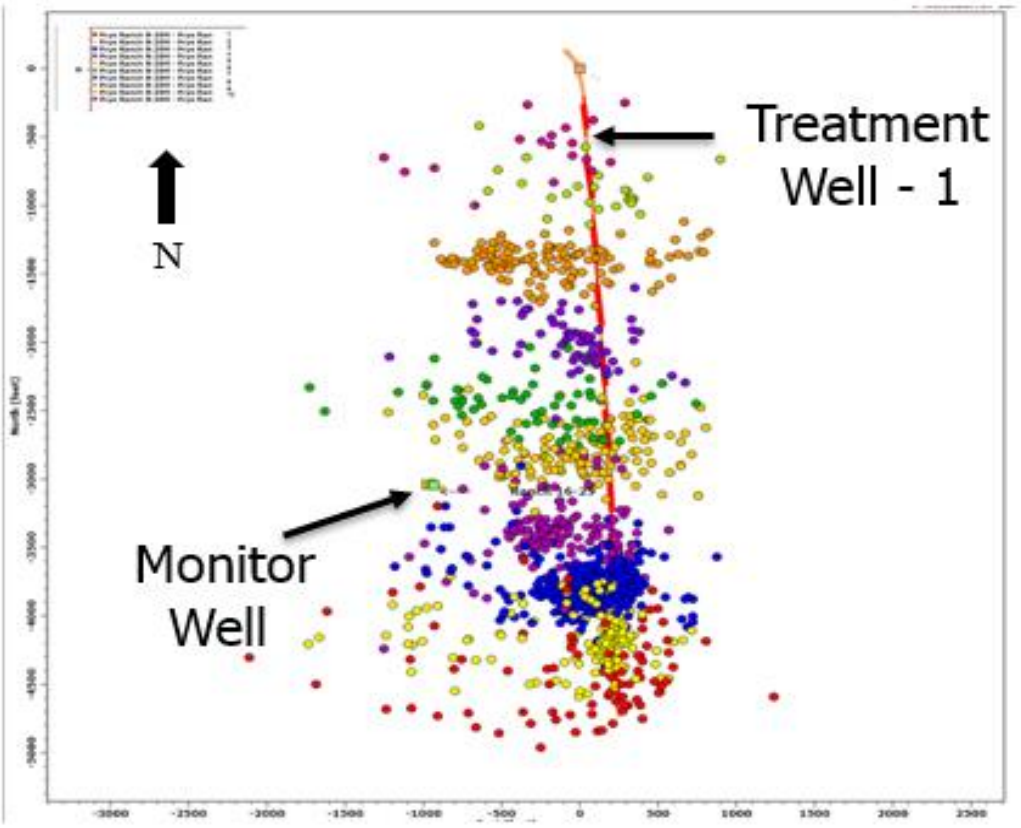

Figure 25: Well-1 microseismic activity top view (Microseismic mapping report)

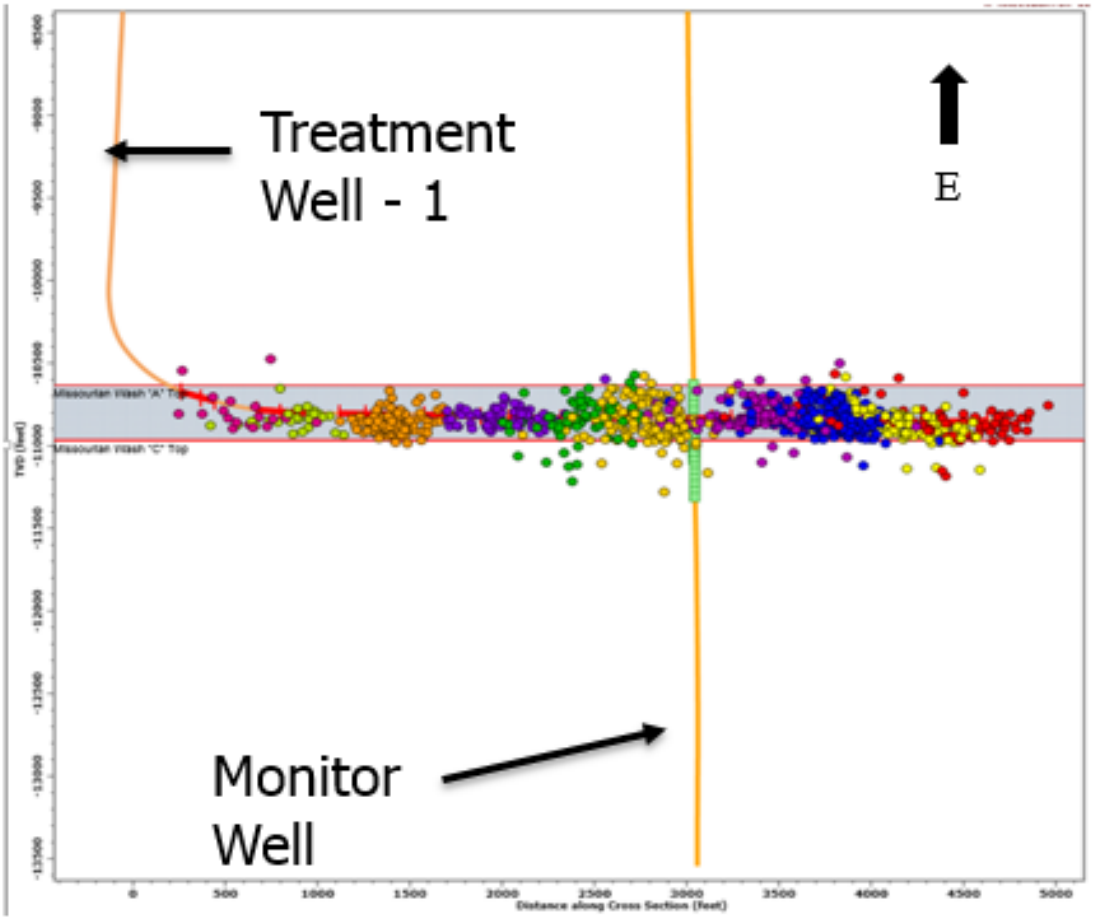

Figure 26: Microseismic scatter side view (Microseismic mapping report)

The report states typical fracture half-lengths of approx. **1000ft,** which seem overly optimistic (wellbore lateral length ≈ 4500ft). High variation in total events mapped across individual stages leads to different confidence levels**.**

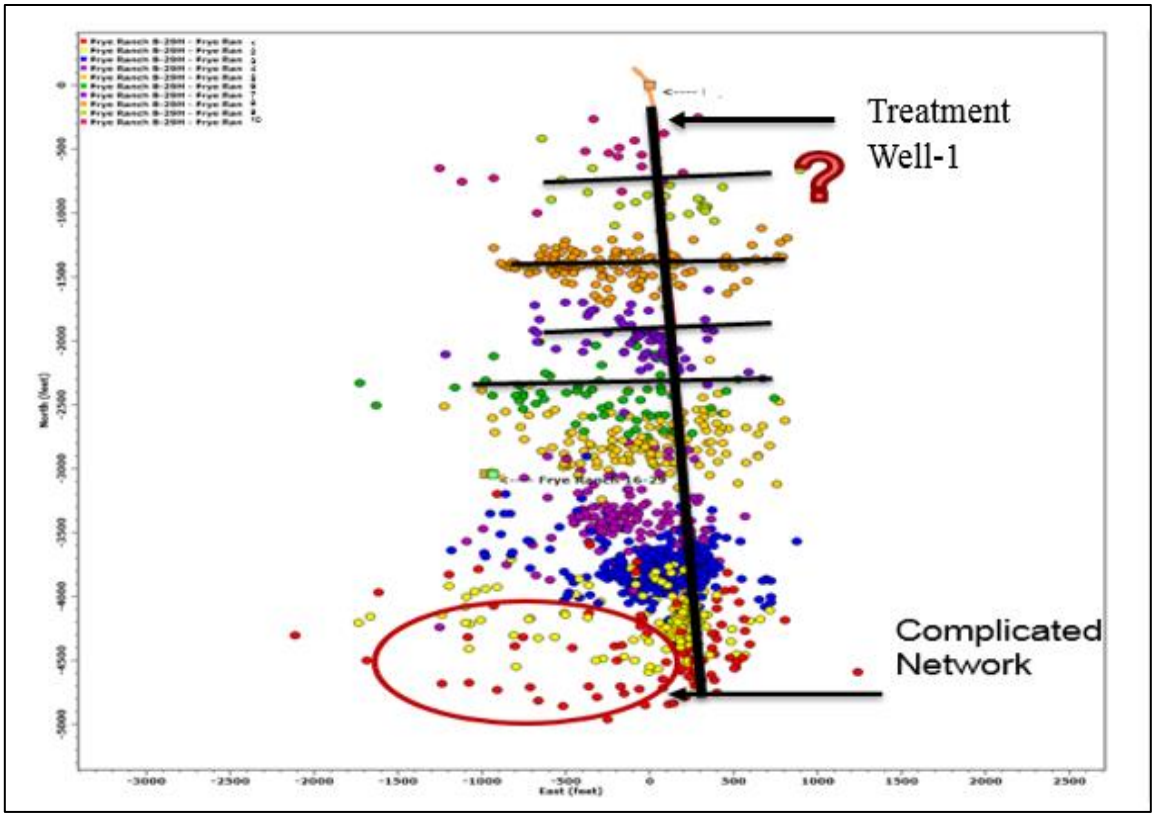

Figure 27: Microseismic report review depicting the complex nature of events detected. An attempt is made to map planar fracture geometry across some stages

Mapping a scattered microseismic activity in a reservoir model is a difficult task without actually possessing the data. As seen in Figure 27 clear planar geometry is not seen in most of the stages. A complicated network of microseismic events is detected near the toe of the well. Also, it is important to ascertain whether a group of microseismic event locations actually relates to parting of rock or is simply a pressure change with little proppant volume involved (Maxwell. 2011).

Amongst all the stages, Stage 3 has the highest number of events mapped during the process. A total of 424 microseismic events are detected across Stage 3 with higher

average confidence level signaling higher signal-to-noise (S/N) ratio. Half-length reported is close to 600ft, which is a realistic estimate for the well. Height is contained within the Wash interval. This stage result was considered the most representative of the expected fracturing activity. Figures 28 and 29 depict the microseismic activity across Stage 3. This stage was considered further for reservoir development and history matching studies.

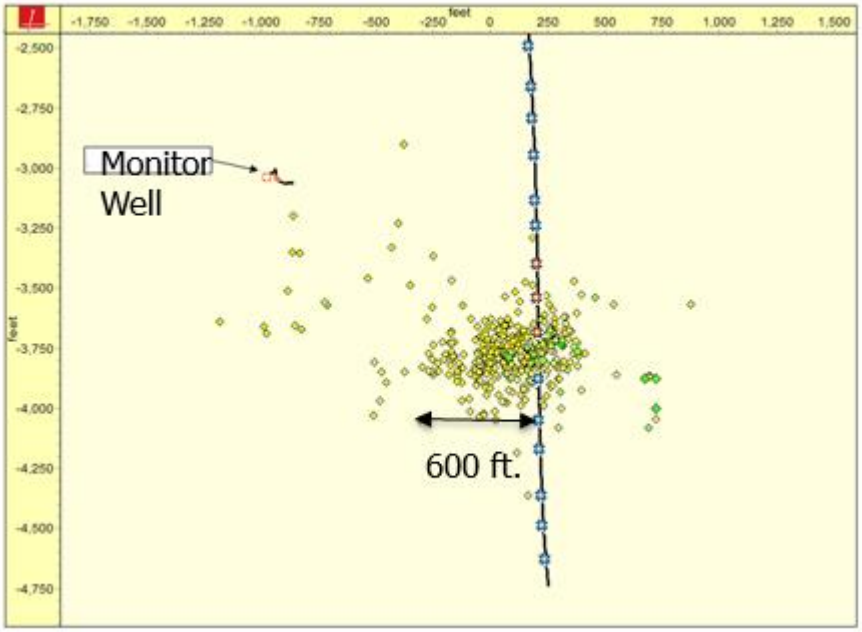

Figure 28: Stage 3 top view of microseismic mapping result, with the extent of major microseismicity

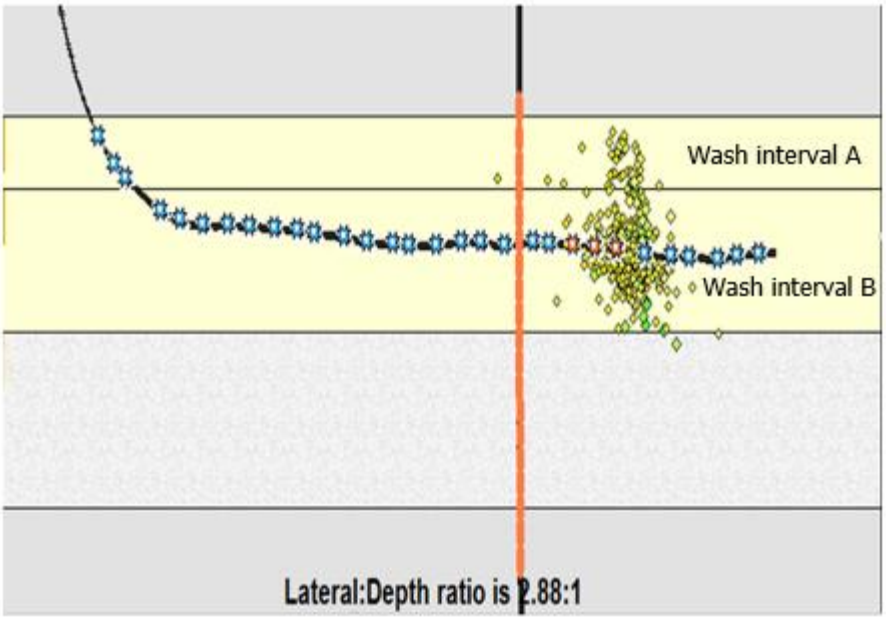

Figure 29: Stage 3 side view of microseismic activity

In unconventional reservoirs, microseismicity provides information to decide if well trajectory is appropriate, whether number of stages and perf clusters are sufficient, and whether fluid pumping rates and volumes are propagating to desired lengths. Even if final fracture dimension estimates are not concrete, microseismic analysis provides valuable information for designing further stimulation treatments.

CHAPTER VII

RESERVOIR MODEL DEVELOPMENT AND SIMULATION

Using the parameters obtained from the earlier analysis, and using reservoir information provided by the operator, a base case reservoir model was setup for the Granite Wash play. The input parameters, model setup and case simulation results are discussed in this chapter. A symmetrical model is extracted from the base model for sensitivity analysis and its validity is proven. Also, sensitivity analysis and history matching parameters are provided. This model is further used in waterflooding simulation.

7.1 Introduction

Unconventional reservoirs have become an increasingly important resource base due to the decline in the availability of conventional resources. The most advanced stimulation techniques need to be applied to these reservoirs with low porosity & permeability, steep pressure declines, and complex reservoir fluid properties. Unconventional tight sand and shale oil reservoirs need stimulated reservoir volume (SRV) created by hydraulic fracturing to let oil or gas flow from matrix to the created fractured network and horizontal well to improve the contact area with the formation (Song et al. 2011). So, horizontal wells with transverse multi-stage fractures induced

assist in economically producing oil and gas from tight reservoirs. Figure 20 shows a visual representation of the process.

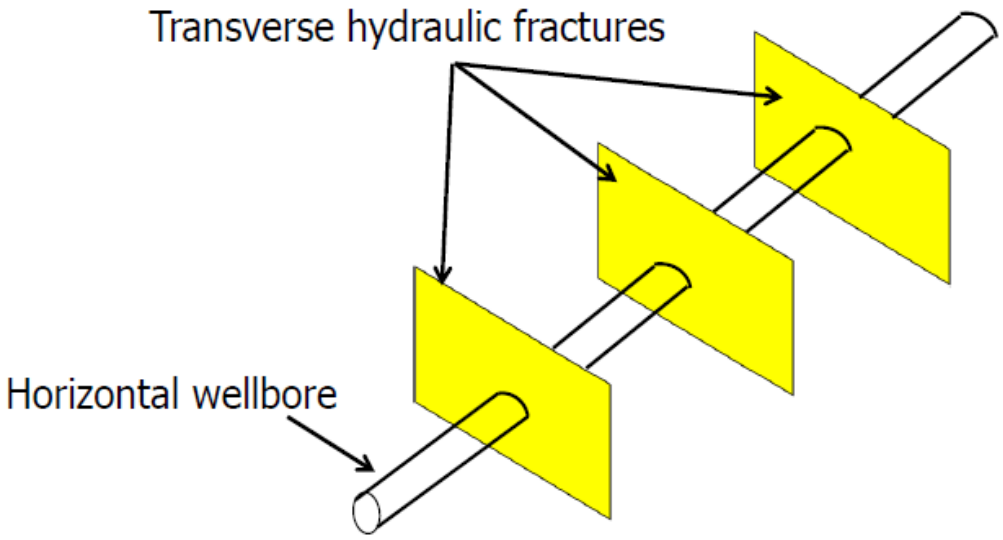

Figure 30: Transverse fractures in a horizontal well (Bo Song et al. 2011)

Rubin (Rubin. 2010), designed an extremely fine grid reference solution which was capable of modeling fracture flow in an unconventional reservoir. The fracture cells were designed to replicate the width of actual fractures (assumed as 0.001 ft.), and flow into the fracture from the matrix using cells small enough to properly capture the very large pressure gradient involved. This process is extremely time consuming if utilized in large fields so a faster reference solution was proposed in his research. Using logarithmically spaced, locally-refined grids represented by 2.0 ft wide cells and keeping original fracture (0.001 ft) conductivity consistent, flow in fractured tight reservoirs can be modeled accurately. The work shows an excellent correlation between an upscaled 2-

ft-fracture coarse model and 0.001 ft wide fracture model. This logarithmically spaced model is more time efficient while also maintaining accuracy in modeling fluid flow in hydraulically fractured reservoirs.

The present research uses the same technique of using logarithmically spaced, locally refined grids around fractures to model fracture flow and consequent pressure and fluid saturation changes.

7.2 Reservoir Model

We developed an isotropic 3-D reservoir well model of the field under consideration. Two horizontal wells with multistage hydraulic fractures were modeled in the field. The dimensions and properties of this model are based on the data provided by the operator. The study area is close to 580 acres so we developed a model 5100 ft. by 4800 ft. Each grid block is of 50ft x 50 ft. dimension. The net pay of the Missourian Wash “B” is close to 50 ft. so 5 layers of 10ft each were modeled in the downward K-direction. This makes it convenient to place the horizontal wellbore in the middle layer and a uniform simulation pattern is obtained. So the base model dimensions are 5100ft x 4800ft x 50ft with 102 x 96 x 5 = 48960 grid cells as seen in figure 31.

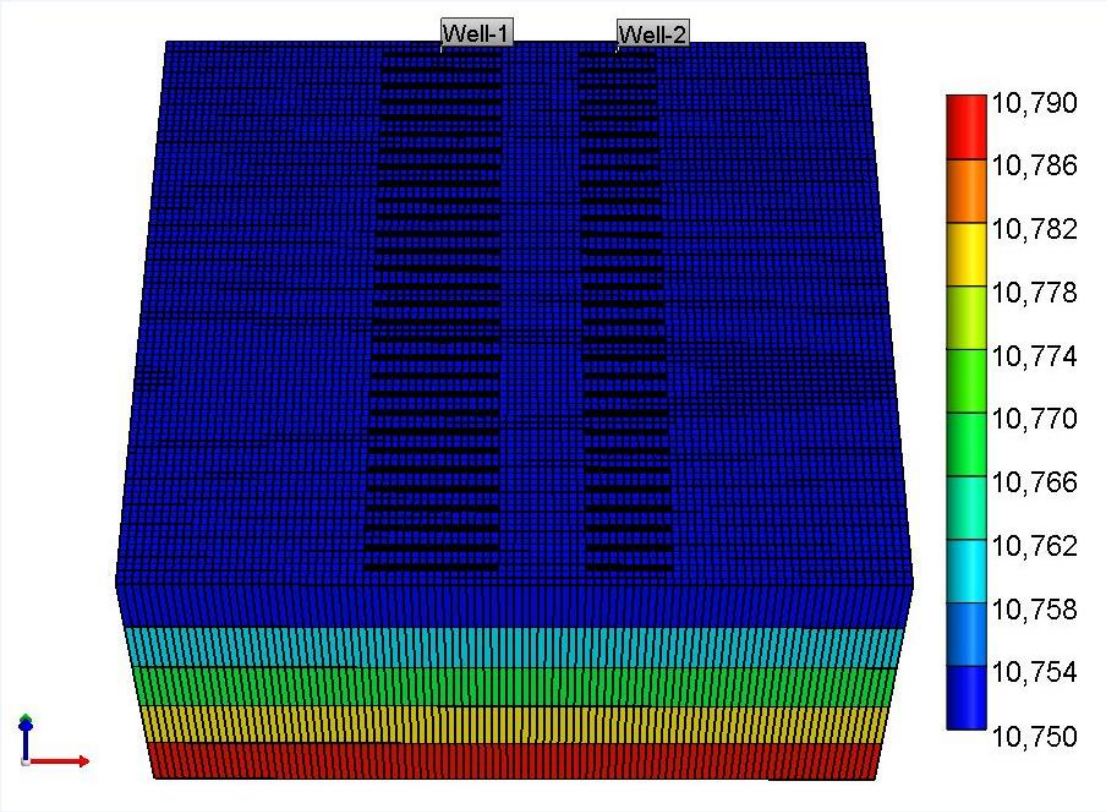

Figure 31: Base reservoir 3-D model

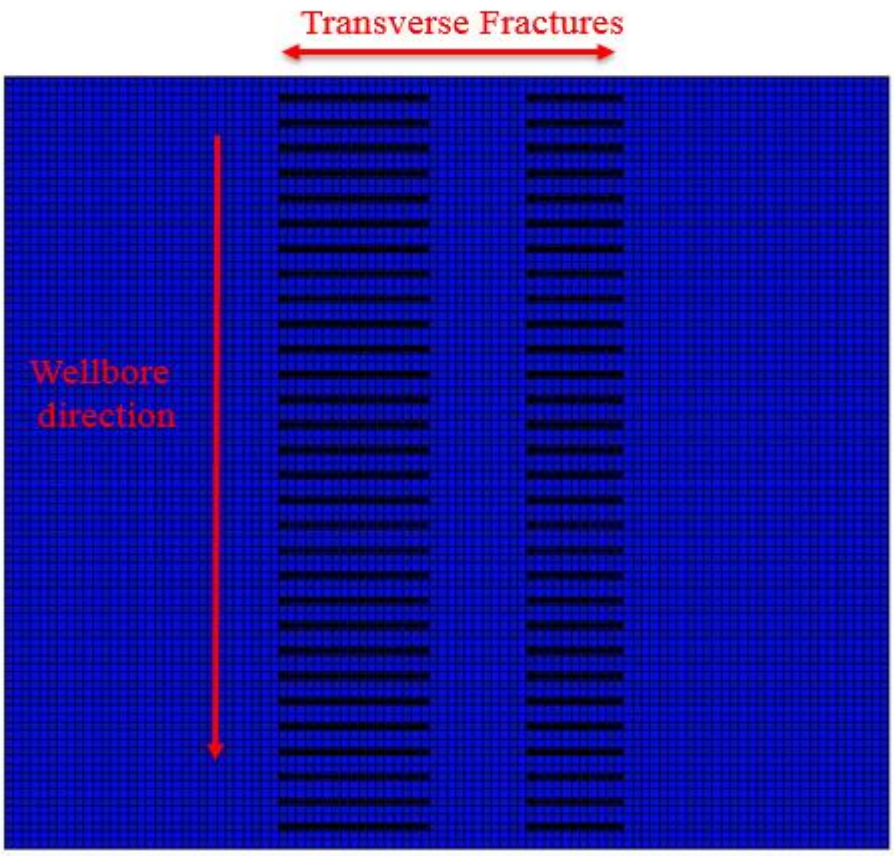

Figure 32: Reservoir model top view

Based on completion reports for Well-1, 3 perforation clusters per hydraulic fracturing stage were utilized and a 10 stage fracturing job was performed. The actual wellbore length is 4450 ft with 10 hydraulic fracturing stages. Based on this, a single stage of 450 ft. was modeled with 3 hydraulic fractures in each stage as seen in figure 33. So the total wellbore length is 4500 ft. which is very close to the actual length of 4450 ft as seen in figure 32. Each hydraulic fracture was further logarithmically gridded in 7 x 7 x1 in the X, Y and Z direction respectively. The logarithmically spaced out grids

accurately model the pressure drop when fluid moves from matrix to the fracture. Figure 34 shows a close-up of a single fracture in both the modeled wells.

As shown by Rubin, running a simulation model with 0.001 ft fracture width is not efficient and time consuming. Hence the fracture cells are scaled to 2.0 ft width and are given the same conductivity as a 0.001 ft fracture. Assuming a 0.001 ft fracture has a permeability of 90,000md, a 2ft fracture would have 45 md permeability and same as the 90md-ft conductivity of 0.001 ft width.

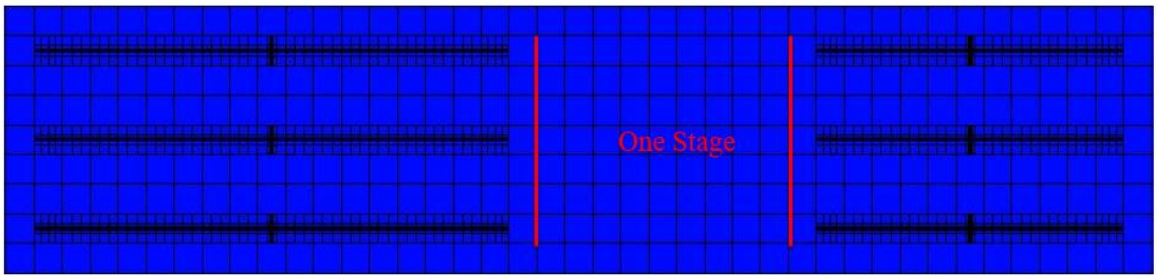

Figure 33: One stage each of Well-1 and Well-2

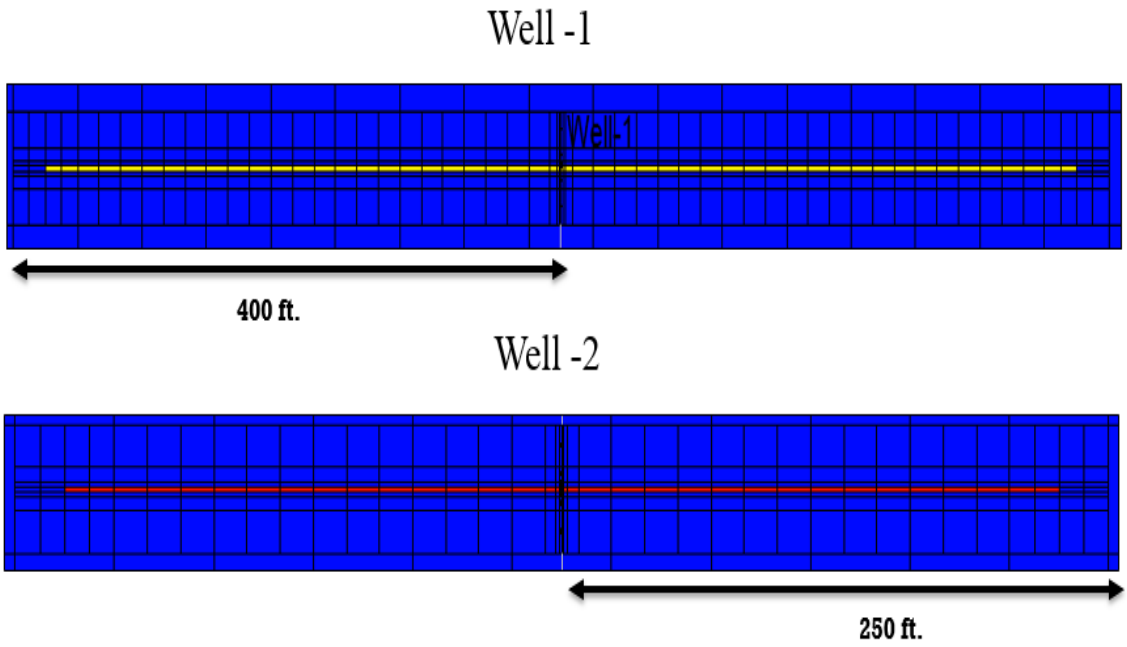

Figure 34: Half-lengths of hydraulic fractures

PVT properties for the model were generated using PVT reports provided. The PVT report contained analysis using separators tests, constant volume depletion and constant composition expansion. These parameters were input in WINPROP module in CMG and the experimental data was matched with fluid behavior trends in the reservoir. Properties such as viscosity, formation volume factors, GORs etc. were matched with change in pressure. The reservoir properties, hydraulic fracture properties, PVT properties and relative endpoints for matrix and fractures are presented later.

Before history matching is performed, sensitivity analysis was performed on some critical parameters. To simplify the computation and work efficiently, a 102 x 9 x 5 = 4590 grid-cells model was built. This symmetry model consists of 3 hydraulic fractures

which corresponds to 1 stage in the base model. This mini symmetry model can be multiplied by a factor of 10 to derive results of running the base model. The reservoir and fracture properties of this model are exactly same as the base model.

7.3 Symmetry Model Validation

Before using the symmetry model for our work, we should test its validity and make sure it mimics the performance of the base model. The symmetry model has the same reservoir, hydraulic fracture, and PVT properties. The base model and the mini symmetry model were run for 30 years at a minimum bottomhole constraint of 2000 psi. As shown in the graph in figure 35, the average reservoir pressure depletion curve and oil recovery factor curve for two models matches perfectly for every time step. Thus, it's accurate to use our symmetry model to evaluate the sensitivity parameters and conduct waterflooding evaluation.

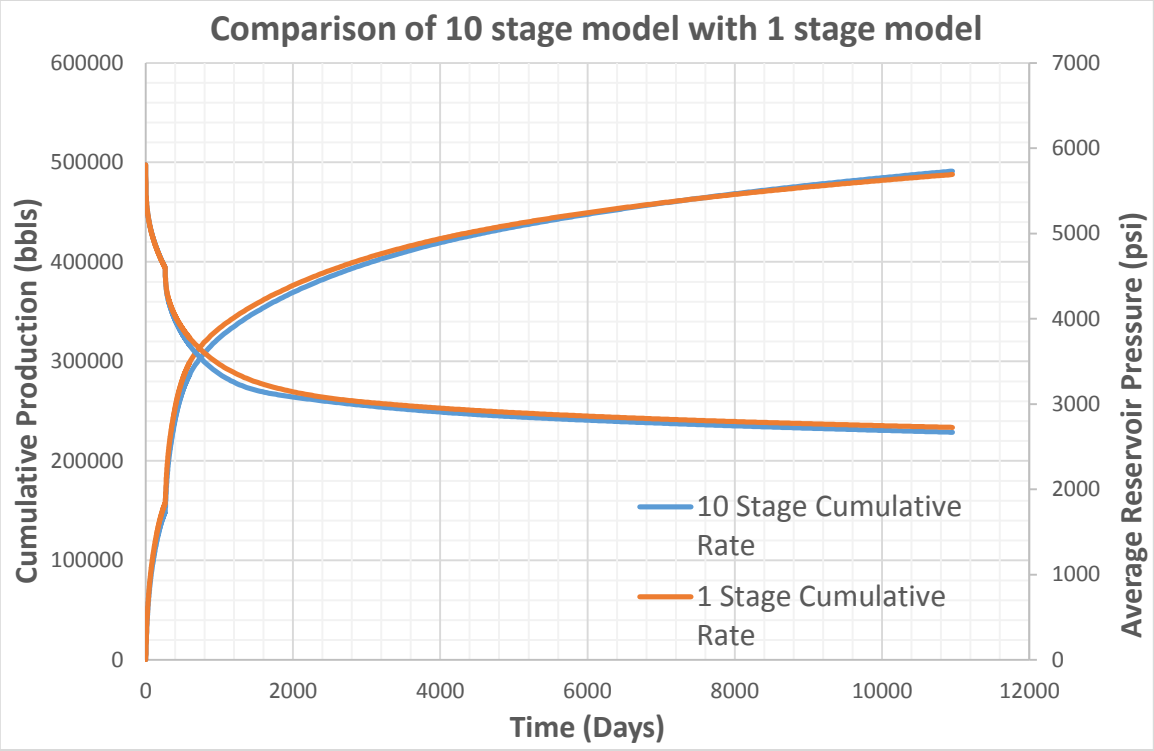

Figure 35: Validation of symmetry model with comparison to actual base model. Average reservoir pressure and cumulative rate are plotted.

7.4 Sensitivity Studies

Sensitivity analysis is a method to quantify the impact of geological and engineering inputs used in a model on the overall reservoir behavior. It is important to identify the important uncertain parameters for the subsequent history matching process. The parameters considered here are fracture half-length, matrix permeability & rock compressibility. The results from the sensitivity studies can be used in not only in understanding of reservoir dynamics but also understanding the fundamental behavior of the tight oil production system.

7.4.1 Fracture Half-Length

The fracture geometry we considered is of planar type fractures due to simulation software constraints and lack of actual microseismic data. The fracture length in our base model is 400 ft. for Well-1 and 250ft. for Well-2. These values were reached upon by analyzing production data and history matching the parameters. Sensitivity analysis of fracture half-length was extremely important before deciding upon ideal fracture half-length.

Fracture half lengths of 500ft, 250ft, 300ft and 350ft were chosen for the sensitivity studies. The plot of average reservoir pressure for different fracture half-length shows that the reservoir pressure decreases faster in case of longer fracture half-length. Longer fracture length means more formation area is exposed to the stimulated reservoir volume leading to more recovery. Higher initial oil production is obtained leading to better ultimate recovery. Figure 36 and Figure 37 show the graphical representation of the same.

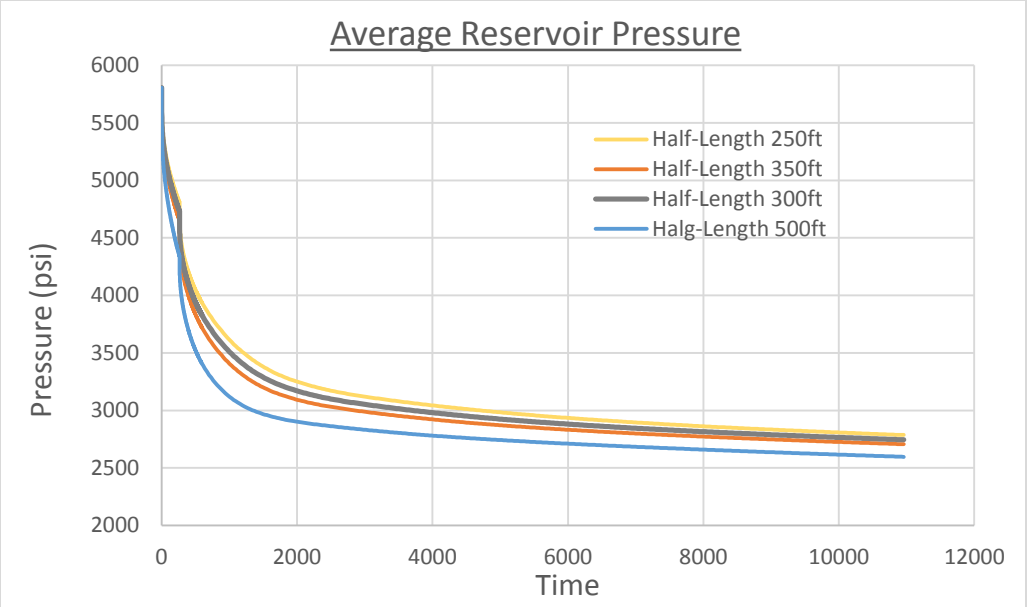

Figure 36: Sensitivity to fracture half-length: average reservoir pressure response to fracture half-length change

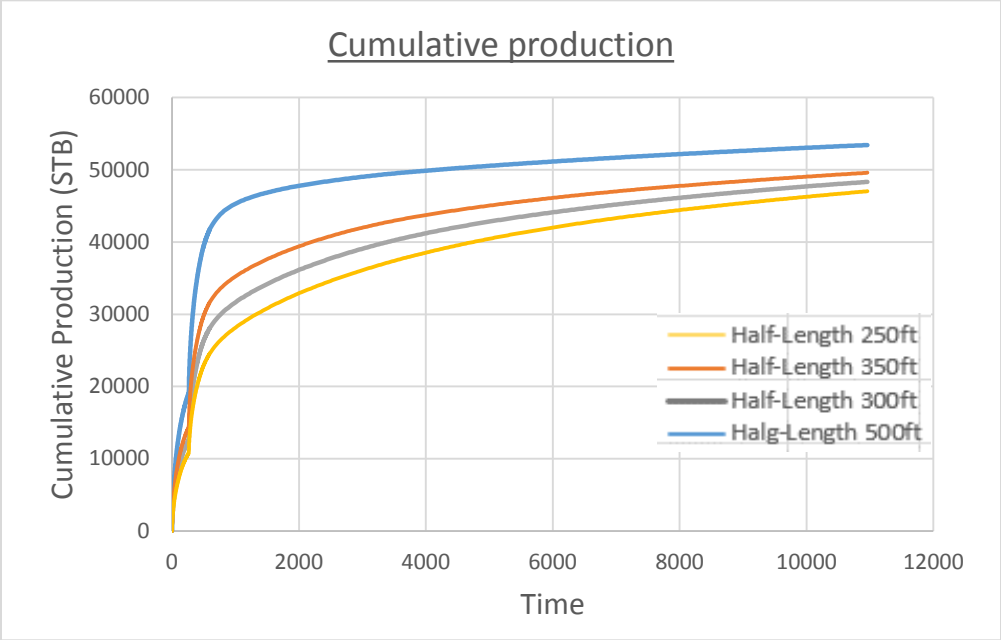

Figure 37: Sensitivity to fracture half-length: cumulative production trends with change in fracture half-length

7.4.2 Matrix Permeability

Flow from a reservoir is a function of extent of interconnected pore space in the rocks. Measuring this permeability accurately is a challenging aspect of developing tight and heterogeneous reservoirs such as the Granite Wash. The conventional ways of determining reservoir permeability like pressure transient testing or formation testing usually do not work in these reservoirs due to very slow response of the formation, and long time intervals are necessary to reach a dependable value of permeability (Mohamed et al. 2011). The DFIT report gave us a reasonable estimate of permeability which we use as a reference point in history matching.

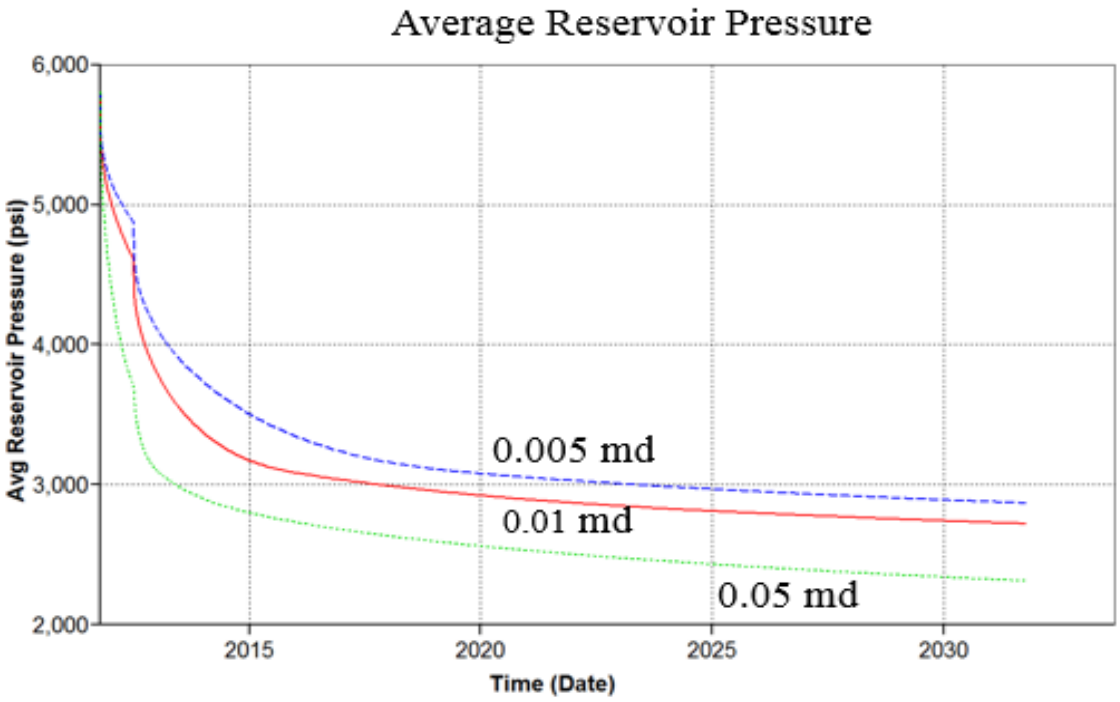

Figure 38: Sensitivity to matrix permeability: average reservoir pressure response

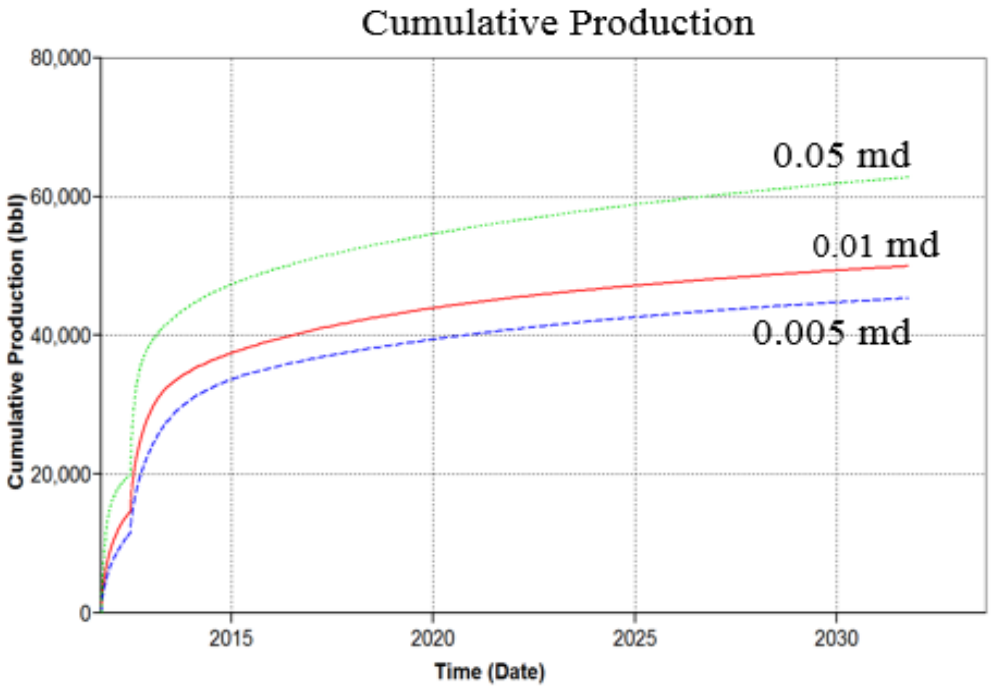

Figure 39: Sensitivity to matrix permeability: cumulative production trends with change in matrix permeability

Permeability values of 0.05md, 0.01md and 0.005md are tested. The reservoir pressure decline is highest for higher permeability and cumulative production is higher as well as seen in figure 38 & figure 39. The matrix permeability is an important parameter and must be determined accurately. The recovery from the formation can highly vary as permeability changes as shown in the study. Thus quantifying matrix permeability is a crucial aspect in reservoir simulation studies.

7.4.3 Rock Compressibility

A reservoir which is tens of thousands of feet below is subjected to overburden pressure due to overlying rock mass. This overburden pressure varies from place to place depending on nature of structure, depth, consolidation and burial history. The compressibility of a hydrocarbon bearing rock is a function of the rate of change of pore volume with change in pressure (Ahmed. 2009). For our base model, we relied on data provided by the operator. The rock compressibility value used in base case is $5.6*10^{-6}$ psi^{-1}. The actual expected compressibility is thought to be on the higher side due to presence of calcite and chlorite in the clay minerals in the formation (Smith et al. 2001).

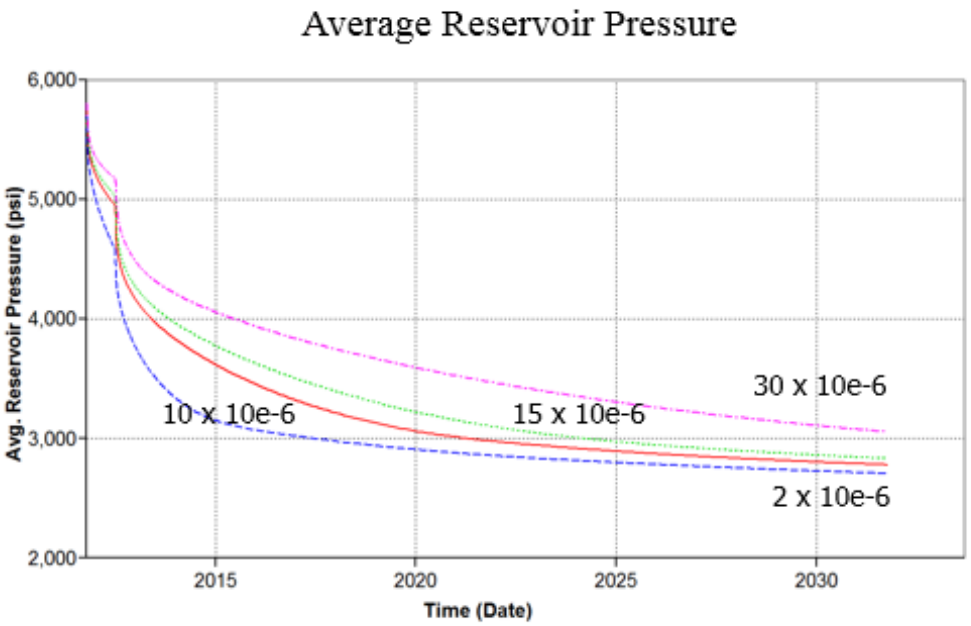

Figure 40: Sensitivity to rock compressibility: average reservoir pressure trends

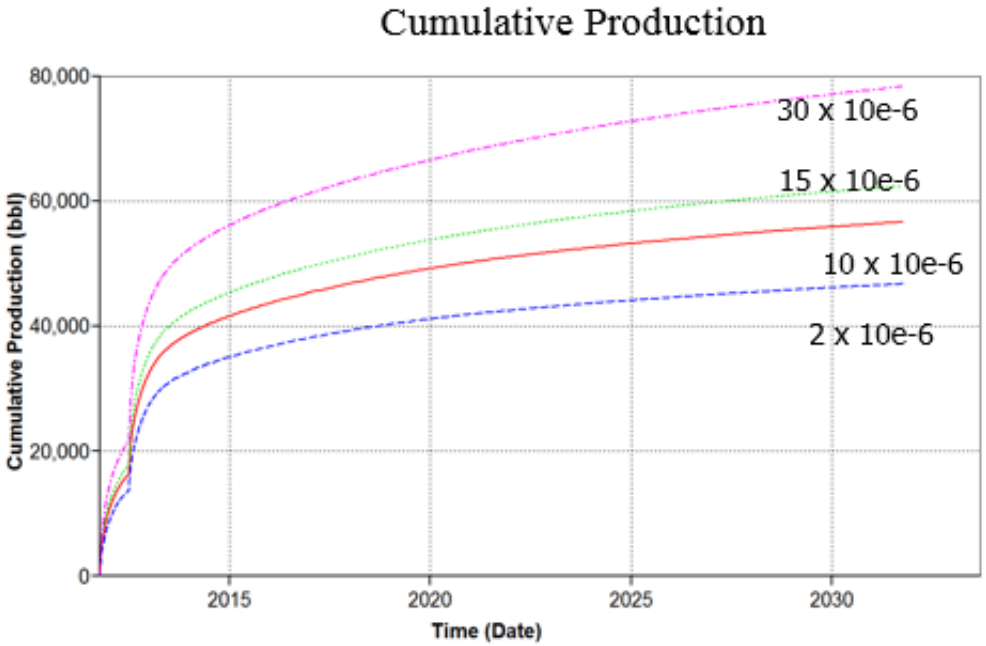

Figure 41: Sensitivity to rock compressibility: cumulative production trends

Rock compressibility values of $2*10^{-6}$, $10*10^{-6}$, $15*10^{-6}$ & $30*10^{-6}$ psi^{-1} are used in the sensitivity analysis. Cumulative recovery can be higher if the rock is found to be more compressible as seen in Figure 40 & figure 41. Reservoir pressure decline is slower if the rock is more compressible according to the study as seen in Fig 40. Laboratory measurements are recommended to determine accurate values of rock compressibility.

7.5 History Match

Based on the sensitivity analysis, history matching was performed on both the wells. The tables 2, 3 & 4 contain the reservoir, PVT and fracture properties.

Table 2: Reservoir Properties of the Granite Wash Formation Field

Initial Reservoir Pressure	5800 psi
Porosity	0.075
Initial Water Saturation	0.32
Compressibility of rock	5.6×10^{-6} psi^{-1}
Permeability	0.009
Reservoir Thickness	50 ft.

Table 3: Fracture Properties of Well-1 and Well-2

Fracture Stages	10 (Each stage containing 3 fractures)
Fracture Spacing	150 ft.
Fracture conductivity	90 md-ft.
Fracture Half-Length	Well-1: 400 ft. Well-2 : 250 ft.
Fracture Cell width	2 ft.

Table 4: PVT Properties of the Reservoir Fluid used in the Simulation Model

Reservoir Temperature	190 F
Saturation Pressure	3732 psi
Initial GOR	1900 scf/stb
°API for oil	42
Gas specific gravity	0.8

The history matching graphs are given below. Oil rate is implemented as primary constraint and a minimum bottomhole constraint of 250 psi is applied. Figure 42 shows the oil rate over the period of available production. Due to the infinite conductivity fractures and steep declines, generating a steady bottomhole pressure profile signals a conducive history match.

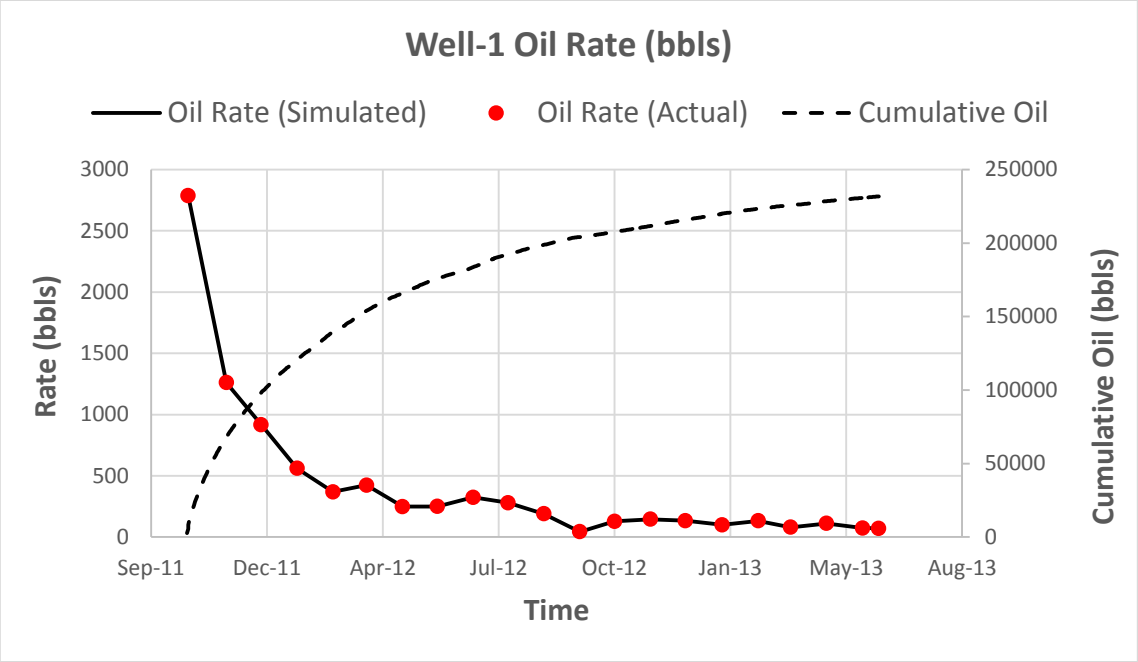

Figure 42: Well-1 historical oil rate

The Gas-Oil ratio (GOR) increases rapidly in Well-1. As fluid moves from the matrix into the highly permeable fractures, the pressure near the hydraulic fractures drops below bubble-point pressure. This causes significant gas production from the initially undersaturated reservoir fluid. The critical gas saturation is kept low so the gas flows up to the surface. Figure 43 shows the simulated GOR trend follows the observed GOR values. The provided production data is highly scattered which may be due to well workover operations, or temporary production shut-ins and restarts. The general trend of increasing GOR is followed.

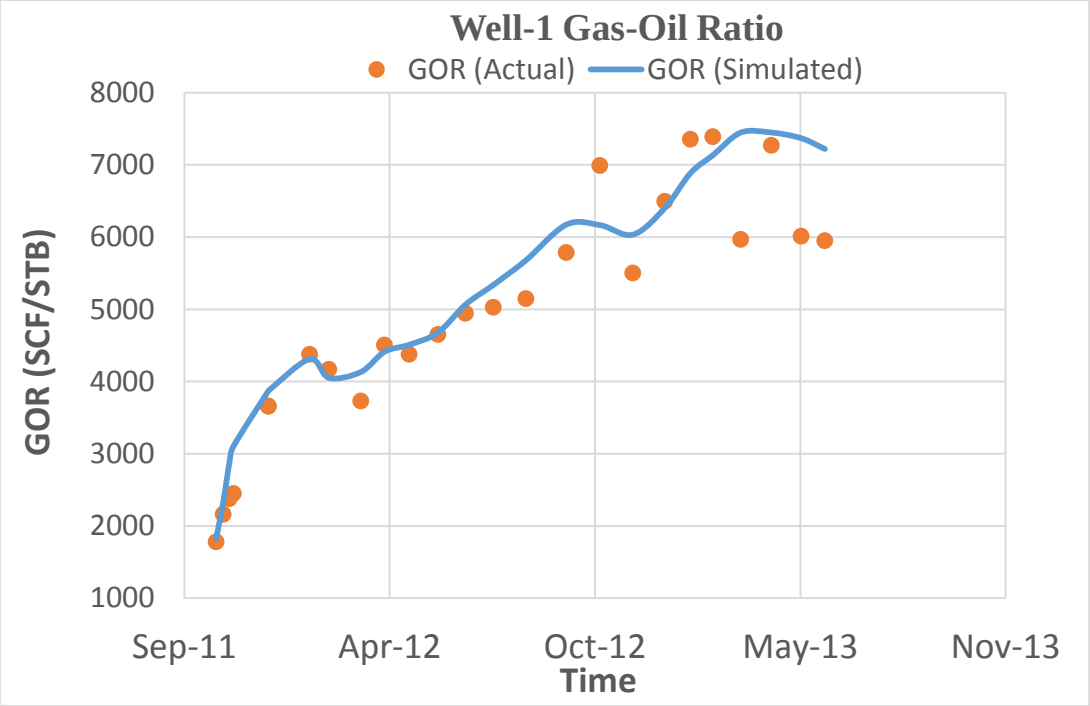

Figure 43: Well-1 field and simulated Gas-Oil Ratio (GOR)

The initial water saturation is 32% throughout the reservoir. As the well is hydraulically fractured, water used for fracturing operations flows-back during initial production time. This generates more water production during initial stages. Similarly, we load our wells with water before start of production in our simulation model. This is achieved by increasing the initial water saturation of the fracture cells in the reservoir model so more water is produced in the initial stages as seen in figure 44.

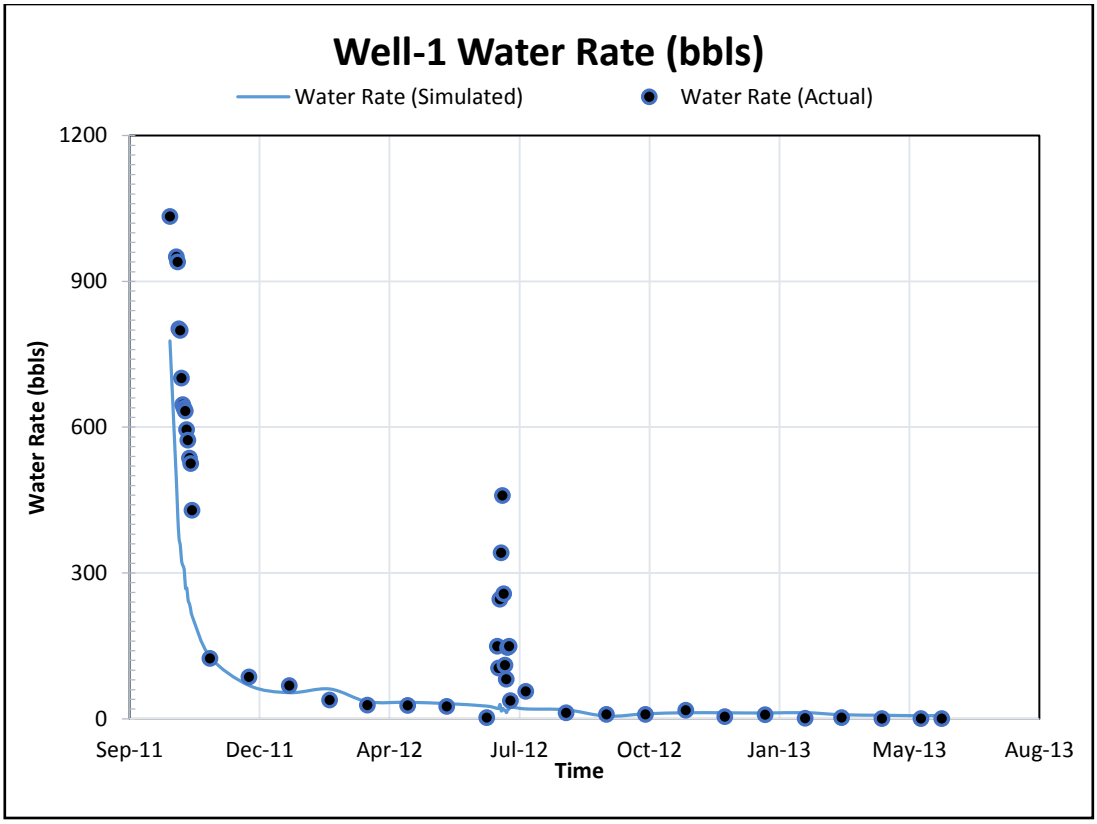

Figure 44: Actual and simulated water-rate profiles of Well-1

Figure 45 shows the bottomhole pressure profile of Well-1. The high initial production rates and increasing GOR signifies a considerable drop in the bottom-hole pressure.

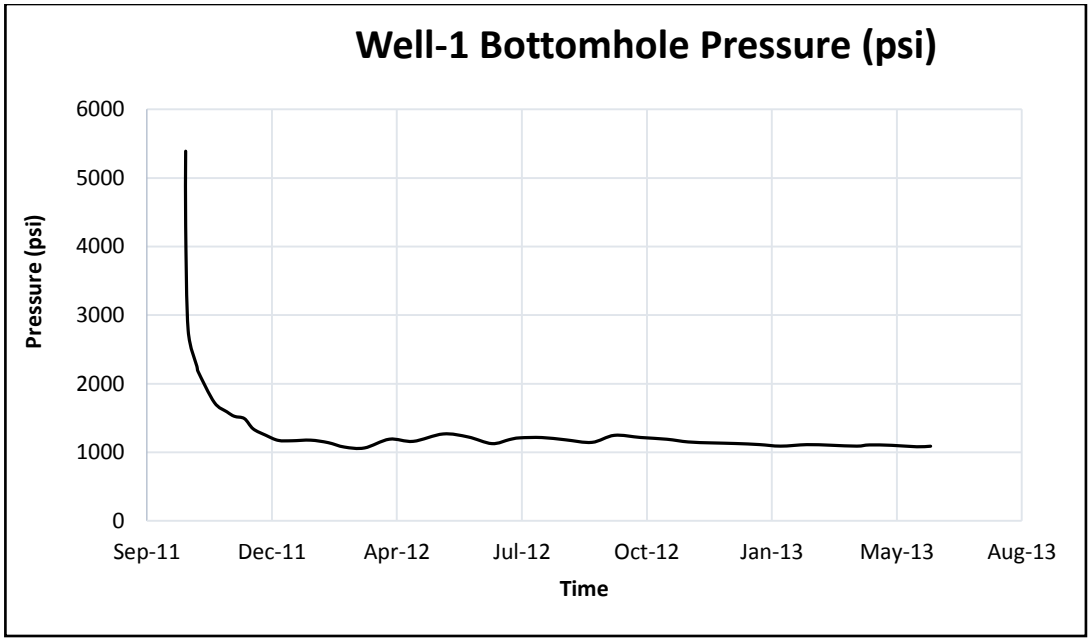

Figure 45: Simulated bottomhole pressure profile of Well-1

As with Well-1, history matching was performed on Well-2 historical production data. Oil rate was the primary matching constraint and GOR and water rates were matched to mimic the actual reservoir depletion profile. Figure 46 shows the historical oil production data that was used to history match the other parameters.

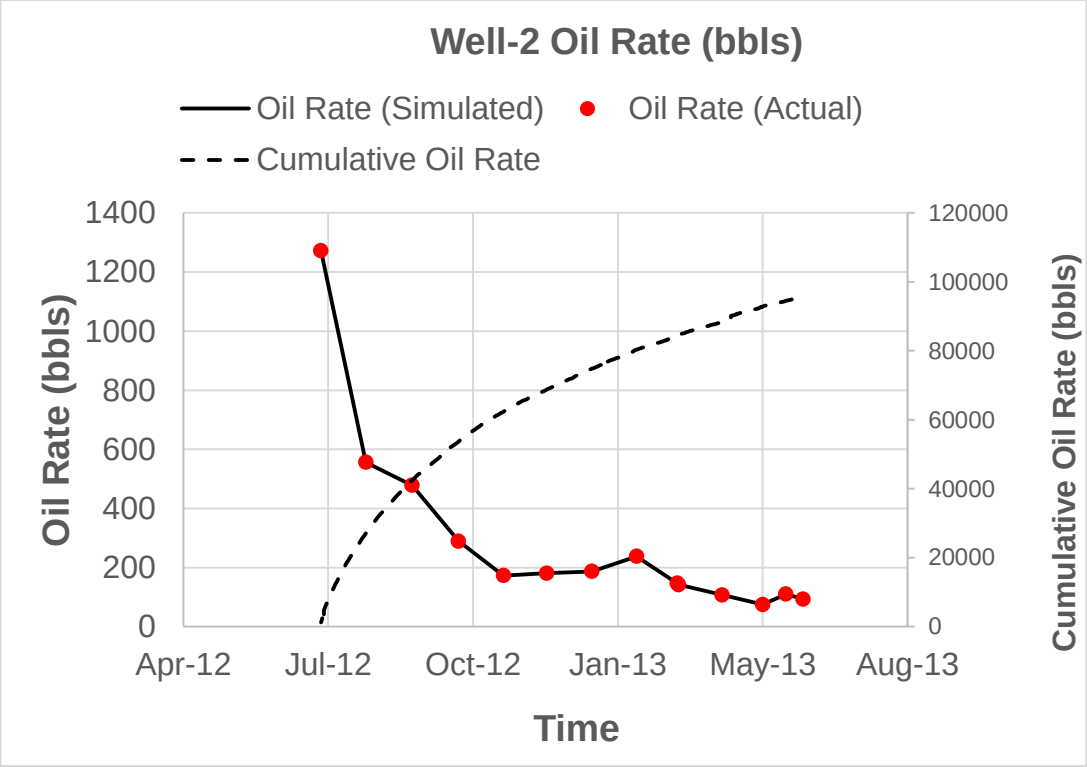

Figure 46: Historical oil-rate of Well-1

Figure 47, figure 48 and figure 49 show the GOR, water and bottomhole pressure matches for Well-2. The increasing GOR trend is observed here as well and the fractures are loaded with water to simulate initial high water production. The bottomhole pressure profile shows a satisfactory trend. It is anticipated that the actual field permeability around Well-2 might be lower due to the lower rate of hydrocarbon returns as compared to Well-1. Another reason might be insufficient stimulation job leading to lower hydrocarbon rate of return. Though for simulation purposes, the overall history match generates comparable and satisfactory results.

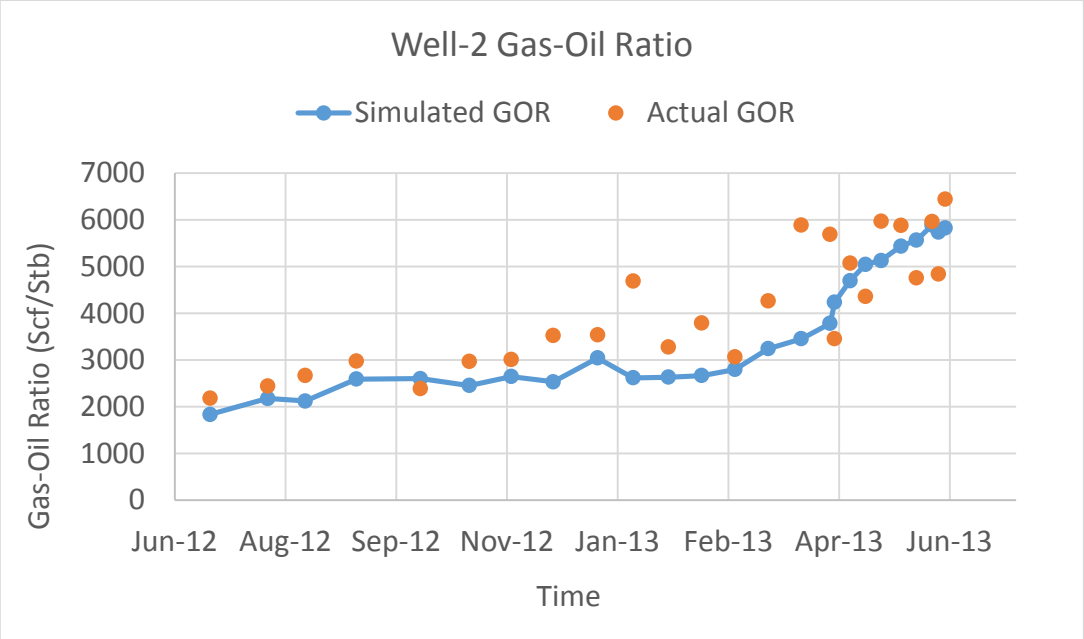

Figure 47: Actual field GOR and simulated GOR comparison

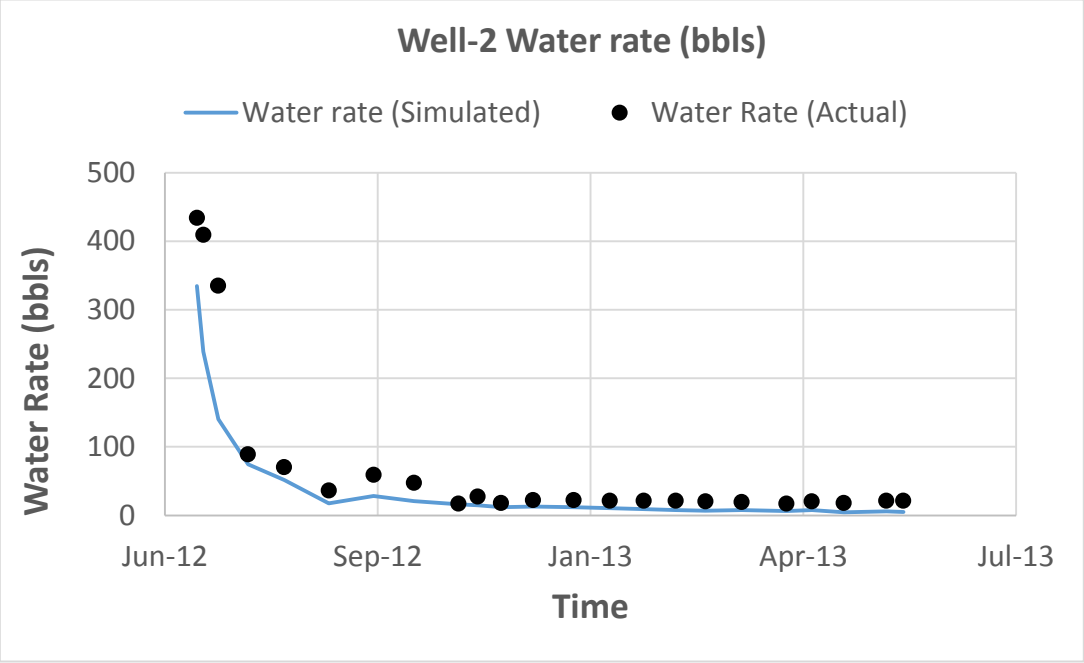

Figure 48: Water-rate history match for Well-2

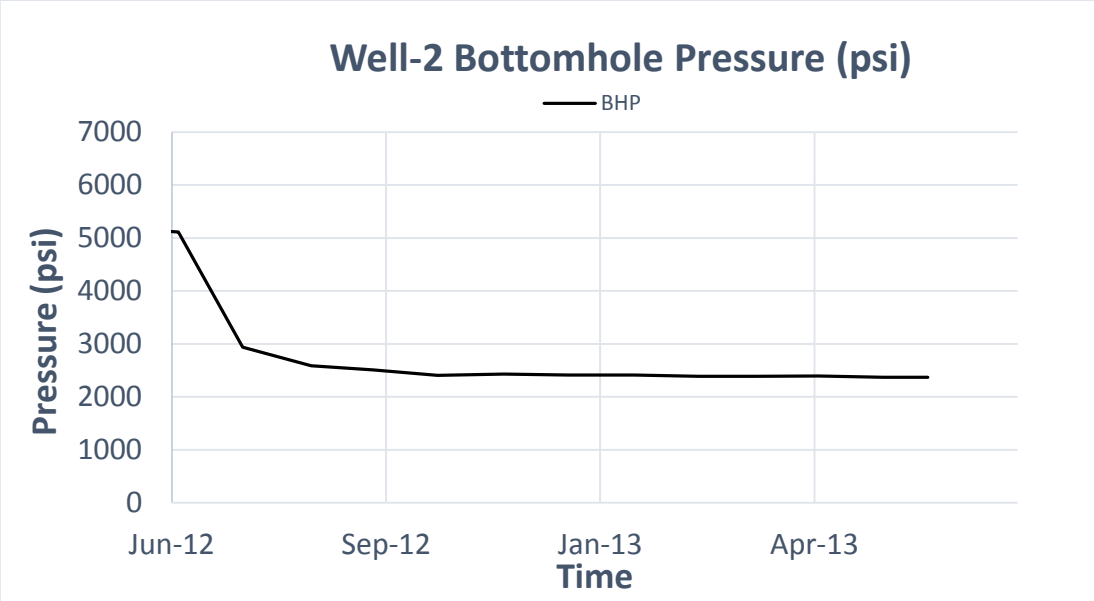

Figure 49: Simulated bottomhole pressure profile of Well-2

CHAPTER VIII

WATERFLOODING TEST AND DEVELOPMENT PLANS

Even after applying advanced horizontal drilling and hydraulic facture techniques in the exploitation of unconventional reservoir, a lot of untapped hydrocarbon resource is left in the reservoir after primary recovery. Understanding reservoir dynamics is critical before enhanced oil recovery techniques such water flooding and gas flooding can be applied in tight reservoirs. After the initial development work, we will now analyze the practicability of applying water injection for pressure maintenance and incremental oil recovery. Water flooding is widely used because water injection is relatively inexpensive, and may be economic despite the low ultimate recoveries obtained. An additional value of water flooding is that, water flooding is a low-risk option that can be used to recover some additional oil while more advanced lab and pilot studies are being designed (Gulick and McCain. 1998). Thus, improving oil recovery by water flooding in reservoirs with remaining residual hydrocarbon saturation is a natural progression of reservoir management. This chapter describes the base water injection model and simulation results of water flooding in the Granite Wash reservoir.

8.1 Description of Waterflooding Model

We used the symmetry model to simulate water injection. Two new horizontal wells, Well-3 and Well-4 were drilled on either side of the original producers and water

flooding was implemented as shown in figure 50. The horizontal wells were drilled in a North-South orientation as well and the half-lengths were 400ft. Distance between the original producers and newly drilled horizontal wells is close to 1000ft. We compare the waterflooding plans with primary recovery achieved after 30 years of natural depletion without any enhanced recovery process. The cumulative production achieved by primary recovery is 763MSTB.

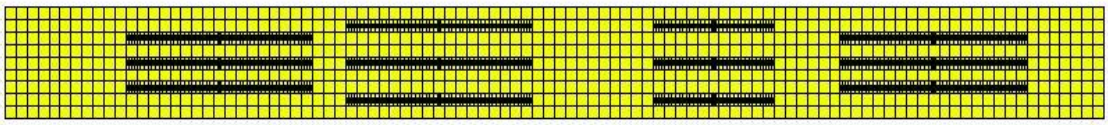

Figure 50: Waterflooding symmetry model description, with two horizontal wells drilled on the exterior side of Well-1 and Well-2

8.2 Water Flooding Plans

The waterflood potential of the field was tested using three water injection plans and cumulative production after 30 years was compared.

8.2.1 Waterflood Plan 1

In production plan 1, we start inject water into reservoir after 3600 days (10 years) of primary production and 20 years of water flooding production is observed. The production is driven by natural pressure depletion in first 10 years. The waterflood recovery is compared to a production plan with no waterflood implementation to

measure the enhanced oil production. The production from primary depletion without waterflooding is 763 MSTB over 30 years resulting in a recovery rate of 14.11%.

When we start water injection, no big differences of production rate can be figured out from the plot of cumulative oil recovered. Because the reservoir has a low permeability, the injection fluid is difficult to transmit from injection well to producer.

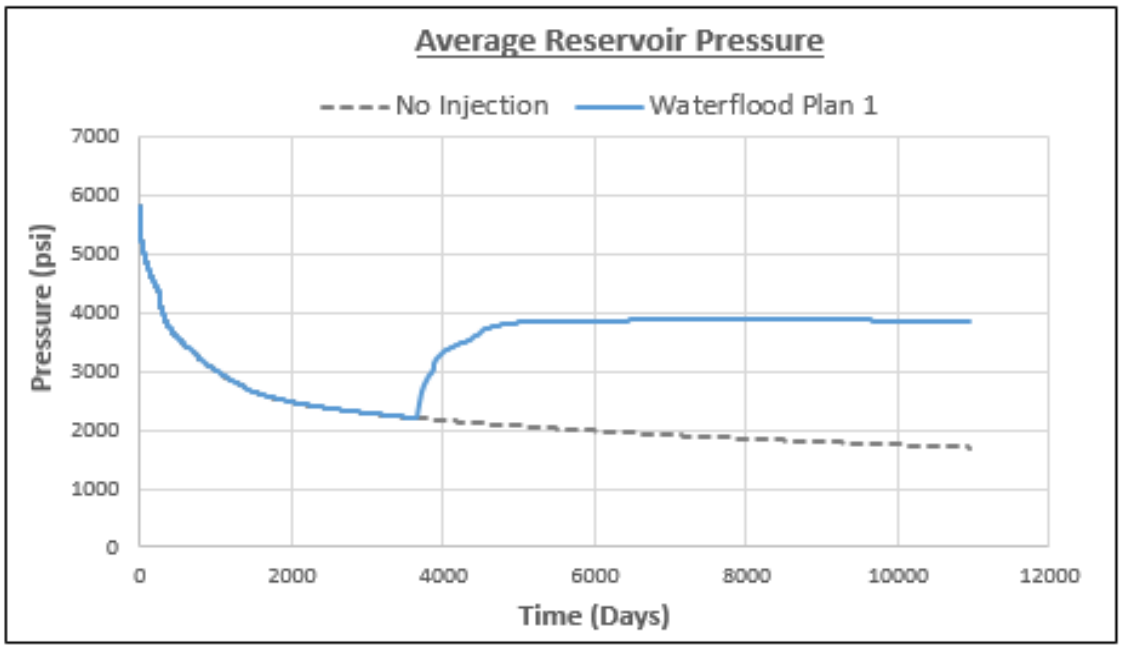

Figure 51: Waterflood plan 1 average reservoir pressure profile

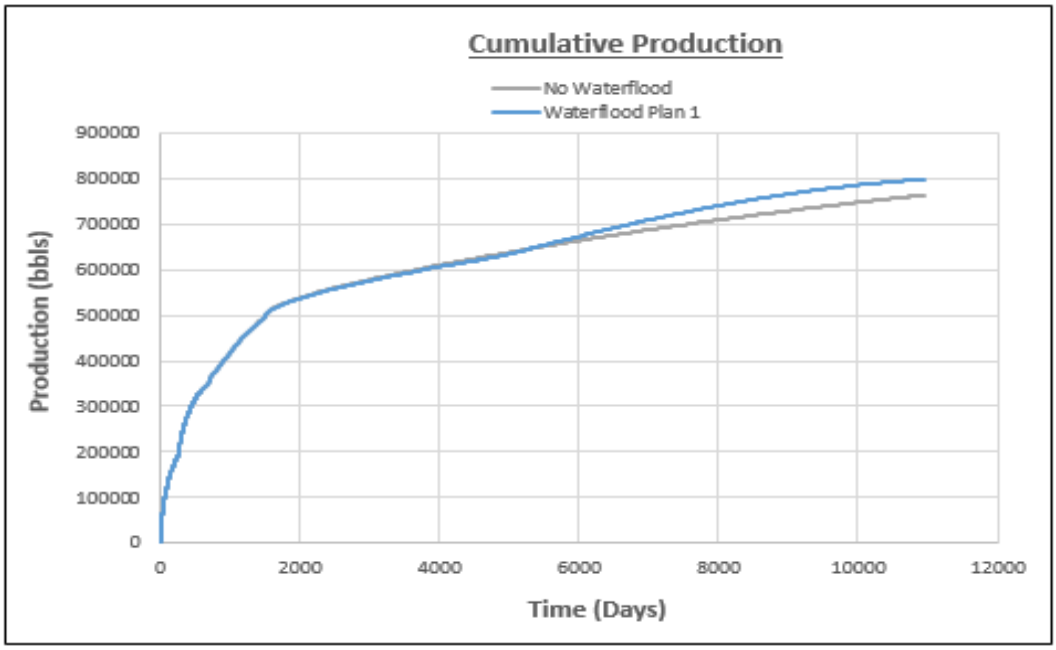

Figure 52: Cumulative oil production of waterflood plan 1

The recovery after 30 years of waterflood is 797 MSTB, accounting for a recovery of 14.9%. This is less than 1% increase than the recovery by primary depletion. Figure 51 and 52 show the average reservoir pressure and cumulative production.

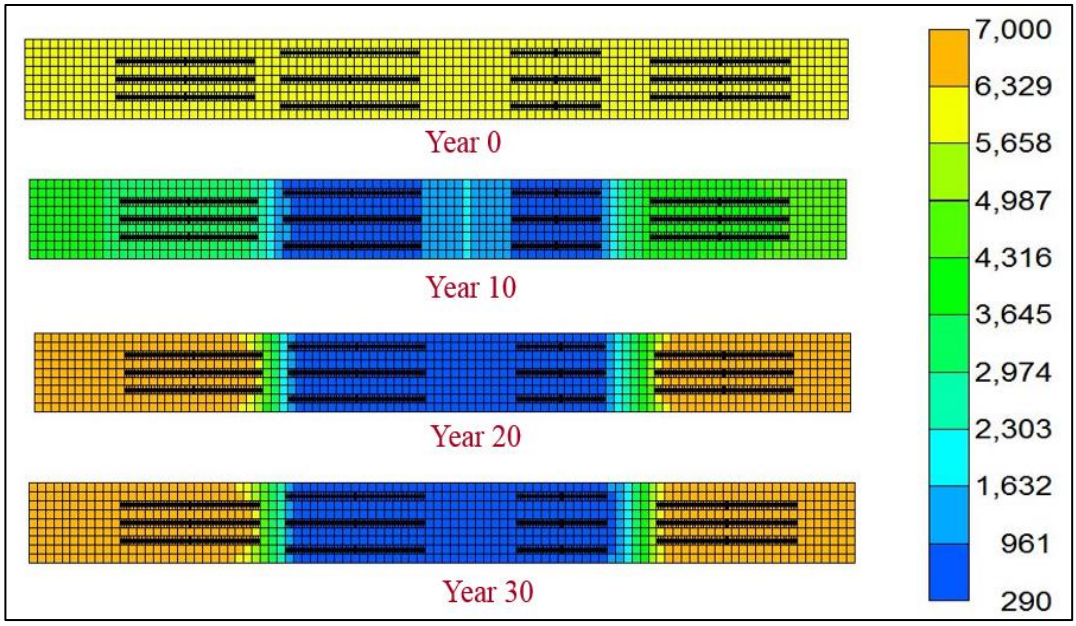

Figure 53: Average reservoir pressure profile as a function of time

Figure 53 shows the average pressure profile over the life of the waterflooding plan. After primary depletion, the pressure close to the well-bore is significantly below the saturation pressure of 3732 psi. After 20 years of water injection, the average reservoir pressure increases but as water does not flood the reservoir efficiently, the pressure around the producing wells remains low. Figure 54 shows the oil saturation as a function of time and water saturation as a function of time.

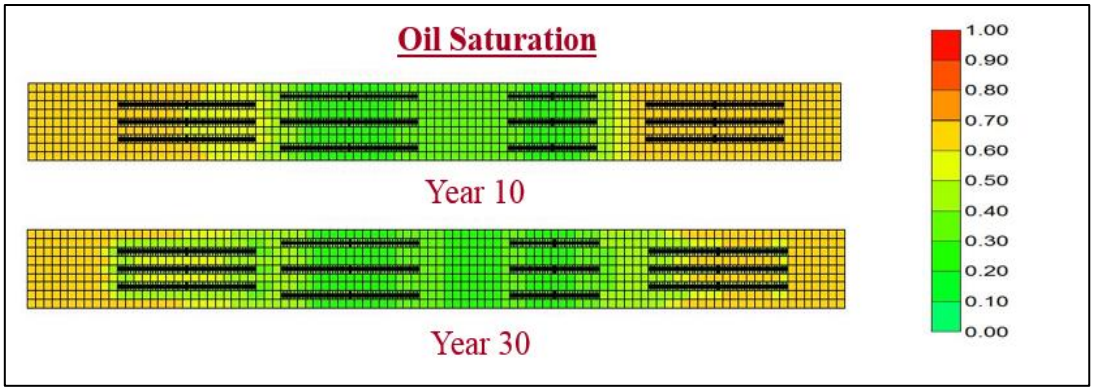

Figure 54: Oil saturation after primary depletion and post-waterflood implementation

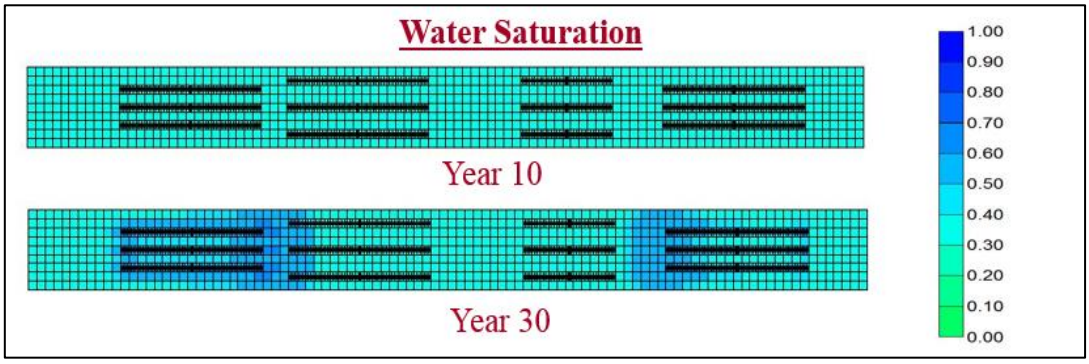

Figure 55: Water saturation profile as a function of time

As seen in Figure 55, the injected water reaches the producing well fractures by the end of 20 years of injection. The added oil recovery from this plan occurs during the time-frame before water reaches the fractures. Due to capillary pressure effects and low permeability, water is unable to sweep large amounts of oil towards the producing wells.

So the cumulative oil production is 797 MSTB and is 34,000 STB higher than the primary recovery plan over 30 years.

8.2.2 Water Flood Plan 2

For production plan 2, we still start water injection after 3600 days (10 years) of primary production. In this plan, we change the injection schedule from constant injection to cyclic injection. Each injection cycle has 5 years' injection and 5 years' shut in period. The idea behind cyclic injection is that the water is imbibed into the formation displacing oil from the pores of the rocks.

As seen in Figure 56, because of cyclic injection, fluctuation occurs in average reservoir pressure curve. Because the tight reservoir has a low permeability, the injection fluid is difficult to transmit from injection well to producer, the response of production well to water flooding is poor, thus oil rate does not have obvious change when start water injection starts. Cumulative production is 776 MSTB which is a recovery of 14.29%, with an incremental recovery of 13,000 STB.

Figure 57 shows the water saturation and oil saturation profiles over the span of waterflood plan-2. The injected water eventually reaches the fractures after recovering a little amount of incremental oil. But as seen in Plan 1, the water does not sweep the oil very effectively due to low matrix permeability and capillary pressure effects. Moreover, the reservoir pressure around the stimulated reservoir volume doesn't increase due to low injectivity leading to poor response to this waterflooding plan.

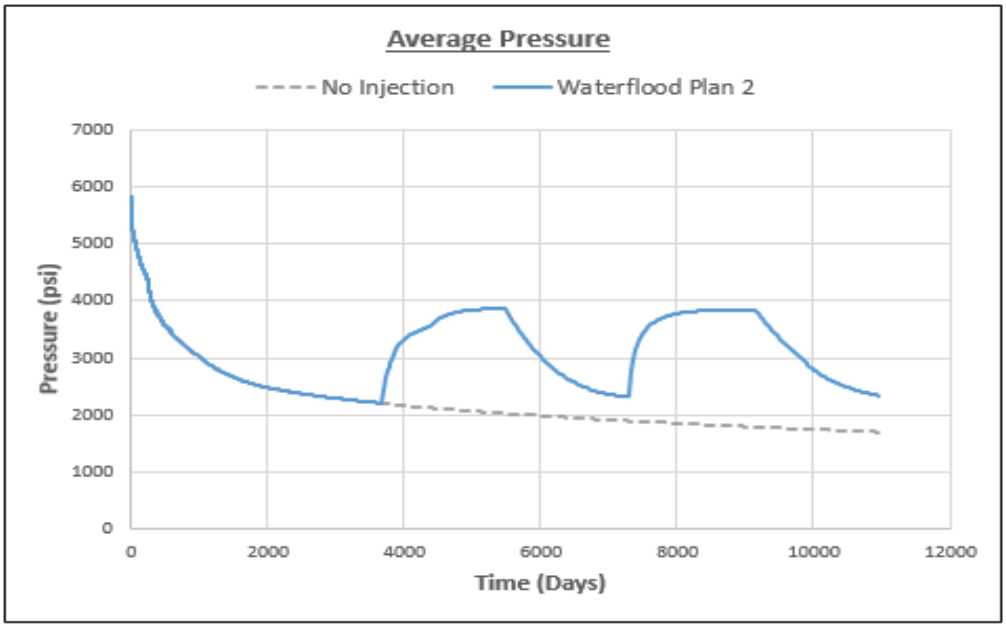

Figure 56: Average reservoir pressure profile for waterflood plan-2

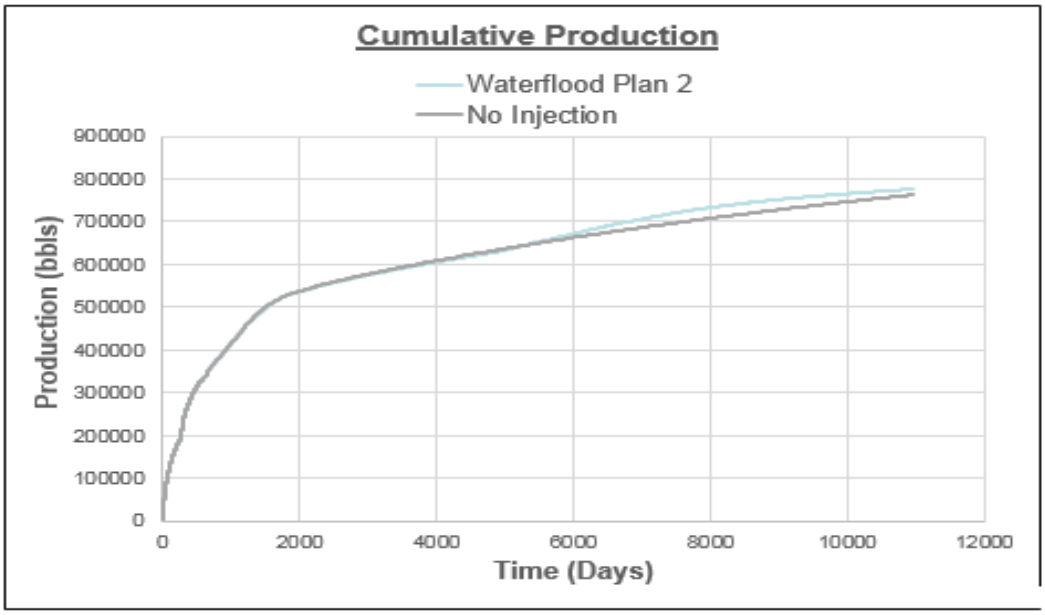

Figure 57: Cumulative production from waterflood plan 2 compared with primary recovery

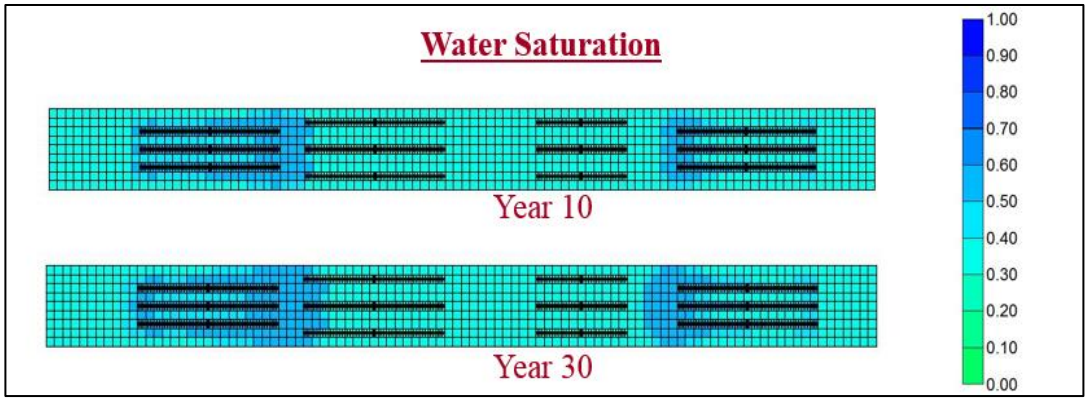

Figure 58: Water saturation profile as a function of time

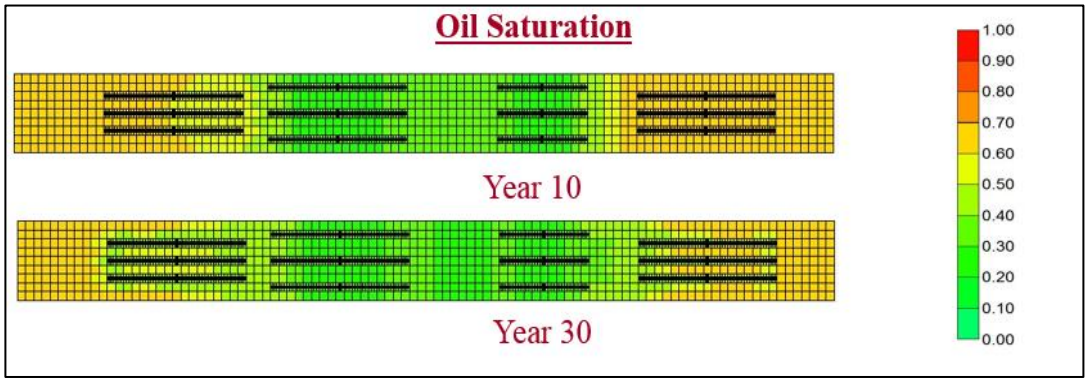

Figure 59: Oil saturation profile as a function of time

8.2.3 Water Flood Plan 3

In plan 3, primary production for 3600 days using 4 horizontals and water injection for 20 years is analyzed. The newly drilled horizontal wells on either side are produced for 5 years and then converted to injectors and waterflooding is initiated for 20 years. Due to the prolonged primary recovery and two added producers, the reservoir is drained more effectively leading to a cumulative production of 1074 MSTB. Afterwards when

water injection is initiated, the water sweeps the remaining oil better and production is increased. The ultimate recovery factor is 20.11%.

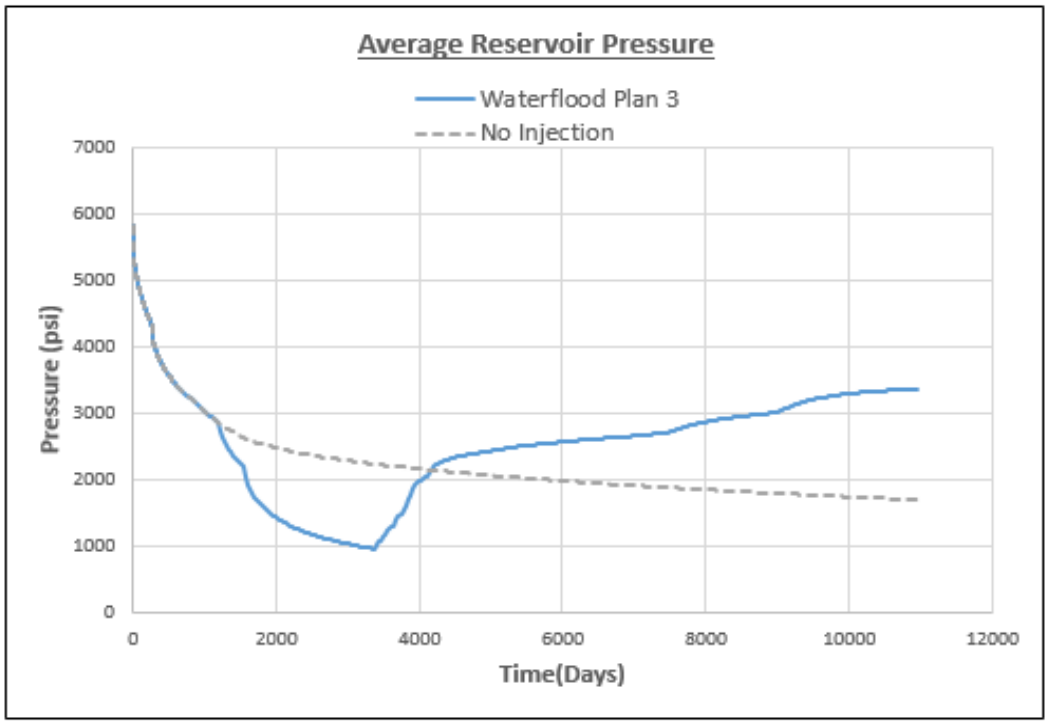

Figure 60: Average reservoir pressure profile for waterflood plan 3

The average reservoir pressure declines even lower due to the additional depletion from the horizontal offset wells. As seen in Figure 61, after 5 years the oil rate shoots up significantly as production from the two new horizontal wells is initiated. The higher oil recovery over the course of the plan is majorly due to production from the offset horizontal wells. A larger reservoir volume is drained as four horizontal wells are used

for hydrocarbon recovery. The incremental oil recovery from the waterflooding that ensues after 10 years when the producers are converted to injectors is not as significant.

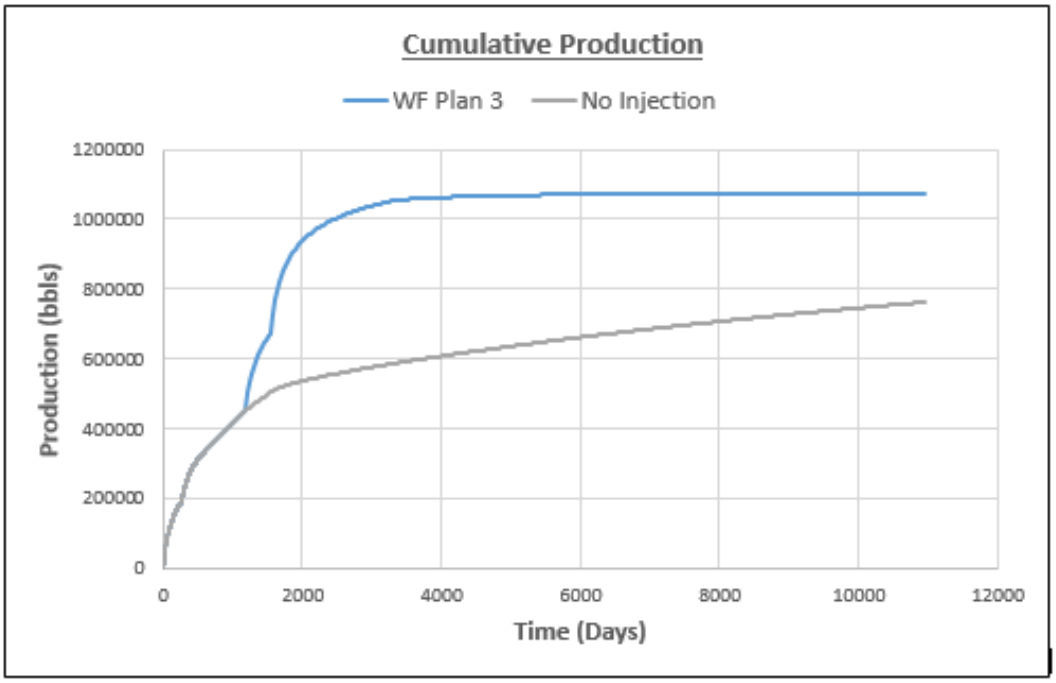

Figure 61: Cumulative oil production from waterflood plan 3

The pressure profiles shown in Figure 62 provide a good overview of the recovery process in this plan. After primary depletion of 10 years, the average reservoir pressure drops down to close to 1500 psi throughout the reservoir. As injection is started, the pressure rises around the injector wells to the constrained maximum injection pressure. The remaining oil is pushed from areas around the injection wells towards producer wells.

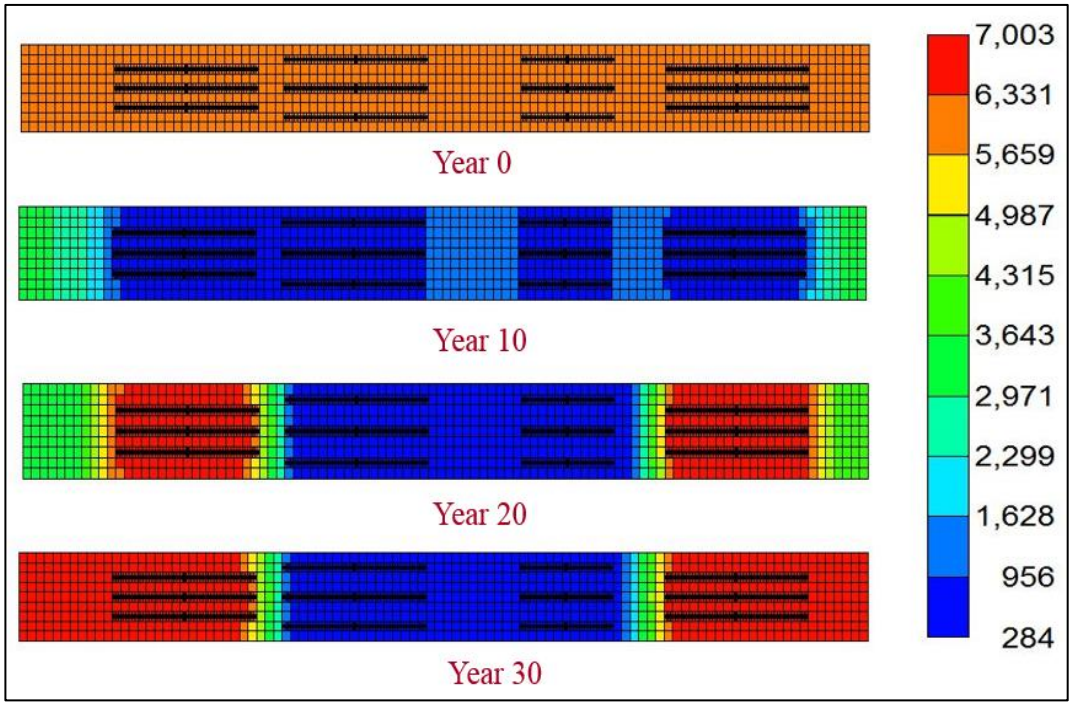

Figure 62: Reservoir pressure profile changes as a function of time

The primary recovery depletes most of the reservoir to close to 35% remaining oil saturation after 10 years. The injected water has more space in the interstices of the rock so water injection is higher in this plan. The added oil recovery from waterflooding is before water enters the fractures of the producing horizontal wells. This phenomenon is commonly known as water breakthrough. Figures 63 and 64 depict the saturation profiles of the reservoir.

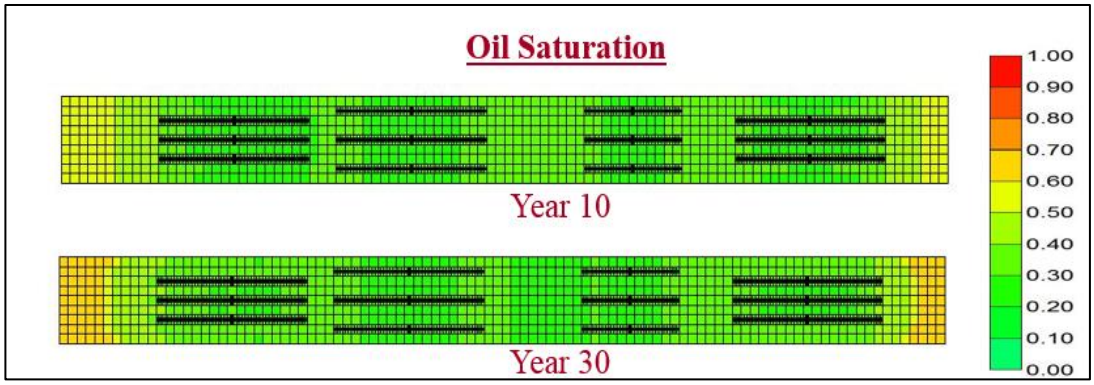

Figure 63: Oil saturation profile map before and after water injection

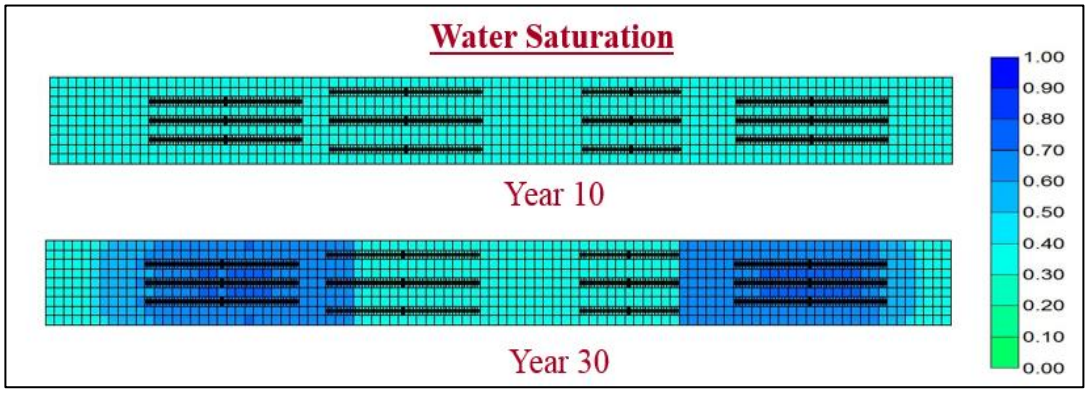

Figure 64: Water saturation profiles before and after injection

8.3 Summary

The Original Oil in Place in the reservoir is 5.34 MMSTB. The following table summarizes the results from the waterflooding recovery plans. It should be noted that the significantly higher oil recovery in Plan 3 is mainly due to implementing production from the offset horizontal wells before starting water injection. A well-spacing pattern of

4 horizontal wells every 600 acres can be implemented in this field to drain the reservoir more effectively. Table 5 summarizes the observed results.

Table 5: Waterflooding Plans Summary

	Plan 1	**Plan 2**	**Plan 3**
Cumulative Oil Production (MSTB)	797	776	1074
Recovery Factor (%)	14.92%	14.53%	20.11%
Injected Water (% HCPV)	21%	19%	36%

CHAPTER IX

CONCLUSIONS AND RECOMMENDATIONS

The oil and gas industry is making tremendous efforts to research on stimulating the oil and gas production from unconventional reservoirs as conventional resources becoming increasingly leaner. The horizontal well with multiple transverse fractures has been long applied for tight oil reservoir production and can be used in the tightest of formations to recover hydrocarbons. But applying secondary recovery processes for tight formations that have been successfully applied to conventional reservoirs will be a great challenge in improving oil recovery. Waterflooding has been successfully implemented in conventional and a few unconventional reservoirs for improving oil recovery. Here we have initiated our work considering feasibility of water injection for improved recovery in the Granite Wash formation.

9.1 Conclusions

1. The Granite Wash is a tight formation with average porosity of 7% and variable clay content. Well-log analysis of the lateral section helps characterize porosity, saturation and clay content.
2. In absence of core data, the Diagnostic Fracture Injection Test & history matching parameters were relied upon for estimating permeability. We

considered an isotropic reservoir with Kx = Ky = 0.009 md for simulation studies.

3. Due to low permeability, water injectivity is generally low and results in poor amount of displaced hydrocarbons on waterflooding. The incremental recovery is less than 1% of OOIP after 20 years of water injection.
4. Drilling closely spaced laterals alongside existing production wells is recommended as it drains the reservoir more effectively. A well spacing of 4 horizontal wells per 600 acre can be utilized. Production rates depend on effectiveness of the hydraulic fracturing job. The transverse hydraulic fracture network of one well should be as close as possible to the fracture network of the adjacent well to maximize recovery, and this can be achieved by longer half-lengths.
5. Hydrocarbon recovery is significantly affected by nature of capillary forces within pores of the rock. This holds true for primary recovery and even more so for displacement carried out by injection of immiscible fluids such as water. Core analysis is necessary for generating dependable capillary pressure relationships.
6. The Diagnostic Fracture Injection Test reports pressure dependent leakoff behavior due to multiple fractures during fracture initiation. This may signal presence of natural fractures in the formation which interact with the propagating hydraulic fractures (Barree et al. 2002). The reservoir should be studied for natural fracture networks before implementing any enhanced recovery process.

7. The wide scatter of microseismic events suggests low stress anisotropy leading to a complex stimulated reservoir volume generation. Lab tests on cores are recommended for accurate interpretation of formation properties affecting fracture propagation.

9.2 Recommendations for Future Work

This study serves as a starting point for analysis of tight formations as candidates for secondary recovery. We recommend an effort to get actual micro-seismic data, transient pressure data, PVT data and core studies data for the liquid-rich Granite Wash intervals. As mentioned before, capillary pressure curves and relative permeability models significantly impact any recovery process from unconventional reservoirs. An in-depth study of these pore-level interactions could shed light on which recovery process can be suitably applied in the Granite Wash formation.

REFERENCES

NEB - Energy Reports- Tight Oil Developments in the Western Canada Sedimentary Basin - Energy Briefing Note. 2014 (3/21/2014).

Ahmed, T. 2009. Working Guide to Reservoir Rock Properties and Fluid Flow: Gulf Professional Publishing: 87-90

Barree, R., Fisher, M. and Woodroof, R. 2002. A Practical Guide to Hydraulic Fracture Diagnostic Technologies. Presented at the SPE Annual Technical Conference and Exhibition, 29 September-2 October, San Antonio, Texas

Cairn, E. 2001. Petrophysical Analysis of Radioactive Sands. Online source: http://www.spec2000.net/18-radsand.htm. Accessed on 02/25/2014

Cooke Jr, C.E. 2005. Method and Materials for Hydraulic Fracturing of Wells. Patent source, Publication Number : US69449491 B2, Date : Sep 27, 2005

Gulick, K.E. and McCain, W. 1998. Waterflooding Heterogeneous Reservoirs: an Overview of Industry Experiences and Practices. Presented at the SPE International Petroleum Conference of Mexico, 3-5 March, Villahermosa, Mexico.

Holditch, S.A. 2006. Tight Gas Sands. Journal of Petroleum Technology 58 (6): 86-93.

Marongiu Porcu, M., Ehlig-Economides, C.A., Economides, M.J. and Retnanto, A. 2014. Comprehensive Fracture Calibration Test Design. Presented at the SPE Hydraulic Fracturing Technology Conference, 4-6 February, The Woodlands, Texas, USA.

Maxwell, S., Shemeta, J., Campbell, E. and Quirk, D. 2008. Microseismic Deformation Rate Monitoring. Presented at the SPE Annual Technical Conference, 21-24 September, Denver, Colorado, USA.

Maxwell, S.C. 2011. What Does Microseismic Tell Us About Hydraulic Fracture Deformation. CSEG Recorder 36 (8): 31-45.

McDaniel, B.W. and Rispler, K.A. 2009. Horizontal Wells with Multi-Stage Fracs Prove to be Best Economic Completion for Many Low-Perm Reservoirs. Presented at the SPE Eastern Regional Meeting, 23-25 September, Charleston, West Virginia, USA.

Miskimins, J.L. 2009. Design and Life-cycle Considerations for Unconventional Reservoir Wells. SPE Production & Operations 24 (02): 353-9.

Mitchell, J. 2011. Horizontal Drilling of Deep Granite Wash Reservoirs, Anadarko Basin, Oklahoma and Texas. Shale Shaker September - October 2011: 118-167

Mohamed, I.M., Azmy, R.M., Sayed, M.A.I., Marongiu-Porcu, M. and Economides, C. 2011. Evaluation of After-closure Analysis Techniques for Tight and Shale Gas Formations. Presented at the SPE Hydraulic Fracturing Technology Conference, 24-26 January, The Woodlands, Texas, USA.

Naik, G. 2003. Tight Gas Reservoirs–An Unconventional Natural Energy Source for the Future. www.sublette-se.org/files/tight_gas.pdf.Accessado 1 (07): 2008.

Nguyen, D.H. and Cramer, D.D. 2013. Diagnostic Fracture Injection Testing Tactics in Unconventional Reservoirs. Presented at the SPE Hydraulic Fracturing Technology Conference, 4-6 February, The Woodlands, Texas, USA.

Nojabaei, B. and Kabir, S. 2012. Establishing Key Reservoir Parameters with Diagnostic Fracture Injection Testing. SPE Reservoir Evaluation & Engineering 15 (05): 563-70.

Rose, S.C., Buckwalter, J.F. and Woodhall, R.J. 1989. The Design Engineering Aspects of Waterflooding: Richardson, TX: Society of Petroleum Engineers: 11-14

Rothkopf, B.W., Christiansen, D., Godwin, H.L. and Yoelin, A.R. 2011. Texas Panhandle Granite Wash Formation: Horizontal Development Solutions. Presented at the SPE Annual Technical Conference and Exhibition, 30 October-2 November, Denver, Colorado, USA.

Rubin, B. 2010. Accurate Simulation of Non Darcy Flow in Stimulated Fractured Shale Reservoirs. Presented at the SPE Western Regional Meeting, 27-29 May, Anaheim, California, USA.

Shah, A., Fishwick, R., Wood, J., Leeke, G., Rigby, S. and Greaves, M. 2010. A Review of Novel Techniques for Heavy Oil and Bitumen Extraction and Upgrading. Energy & Environmental Science 3 (6): 700-14.

Smith, P., Hendrickson, W. and Woods, R. 2001. Comparison of Production and Reservoir Characteristics in “Granite-Wash” fields in the Anadarko Basin. Presented at the Petroleum Systems of Sedimentary Basins in the Southern Midcontinent, 2000 symposium: Oklahoma Geological Survey Circular.

Song, B., Economides, M.J. and Ehlig-Economides, C.A. 2011. Design of Multiple Transverse Fracture Horizontal Wells in Shale Gas Reservoirs. Presented at the SPE Hydraulic Fracturing Technology Conference, 24-26 January, The Woodlands, Texas, USA.

Srinivasan, K., Dean, B.K., Azmi, Z.M. and Belobraydic, M. 2013. Evolution of Horizontal Well Hydraulic Fracturing in the Granite Wash-Understanding Well Performance Drivers of a Liquids-Rich Anadarko Basin Formation. Presented at the SPE Hydraulic Fracturing Technology Conference, 4-6 February, The Woodlands, Texas, USA.

Srinivasan, K., Dean, B., Olukoya, I. and Azmi, Z. 2011. An Overview of Completion and Stimulation Techniques and Production Trends in Granite Wash Horizontal Wells. Presented at the SPE Americas Unconventional Gas Conference 2011, 14-16 June, The Woodlands, Texas, USA.

Strickland, B.D., Purvis, D.L., Cox, S.A., Brinska, J.C. and Barree, R.D. 2003. Analysis of Stimulation Effectiveness in the Ammo Field Granite Wash Based on Reservoir Characterization & Completion Database. Presented at the SPE Production and Operations Symposium, 23-26 March, Oklahoma City, Oklahoma, USA.

Warpinski, N. 2009. Microseismic Monitoring: Inside and out. Journal of Petroleum Technology 61 (11): 80-5.

Warpinski, N. WSL, and CA Wright (2001). Analysis and Prediction of Microseismicity Induced by Hydraulic Fracturing, SPE 71649. SPE Annual Technical Conference and Exhibition, 30 September-3 October, New Orleans, Louisiana.